HHS Public Access

Author manuscript

Neurobiol Learn Mem. Author manuscript; available in PMC 2022 January 01.

Published in final edited form as:

Neurobiol Learn Mem. 2021 January ; 177: 107358. doi:10.1016/j.nlm.2020.107358.

Disruption of rat deep cerebellar perineuronal net alters eyeblink conditioning and neuronal electrophysiology

Deidre E. O'Dell[*], **Bernard G. Schreurs**, **Carrie Smith-Bell**, **Desheng Wang**

Department of Neuroscience, Rockefeller Neuroscience Institute, WVU, 33 Medical Center Dr, Morgantown, WV 26505, United States

Abstract

The perineuronal net (PNN) is a specialized type of extracellular matrix found in the central nervous system. The PNN forms on fast spiking neurons during postnatal development but the ontogeny of PNN development has yet to be elucidated. By studying the development and prevalence of the PNN in the juvenile and adult rat brain, we may be able to understand the PNN's role in development and learning and memory. We show that the PNN is fully developed in the deep cerebellar nuclei (DCN) of rats by P18. By using enzymatic digestion of the PNN with chondroitinase ABC (ChABC), we are able to study how digestion of the PNN affects cerebellar-dependent eyeblink conditioning in vivo and perform electrophysiological recordings from DCN neurons in vitro. In vivo degradation of the PNN resulted in significant differences in eyeblink conditioning amplitude and area. Female animals in the vehicle group demonstrated higher levels of conditioning as well as significantly higher post-probe conditioned responses compared to males in that group, differences not present in the ChABC group. In vitro, we found that DCN neurons with a disrupted PNN following exposure to ChABC had altered membrane properties, fewer rebound spikes, and decreased intrinsic excitability. Together, this study further elucidates the role of the PNN in cerebellar learning in the DCN and is the first to demonstrate PNN degradation may erase sex differences in delay conditioning.

Keywords

PNN; DCN; Electrophysiology; Eyeblink conditioning; ChABC

1. Introduction

Nervous system function is centered on neurons, but these neurons are modulated by many external factors including other cells like glia and even the extracellular matrix (ECM) (Araque et al., 1999; Brückner et al., 1993; Cope & Gould, 2019; Ferrer-Ferrer & Dityatev, 2018; Perea et al., 2009; Rakic, 1971). Although there are multiple types of ECM, a specialized ECM structure called the perineuronal net (PNN) plays a key role in myriad

[*]Corresponding author at: Department of Neuroscience Rockefeller Neurosciences Institute, WVU 33 Medical Center Dr, Morgantown, WV 26505, United States. deodell@mix.wvu.edu (D.E. O'Dell).

CRediT authorship contribution statement

Deidre E. O'Dell: Investigation, Writing - original draft. **Bernard G. Schreurs:** Supervision, Writing - review & editing. **Carrie Smith-Bell:** Validation, Writing - review & editing. **Desheng Wang:** Investigation, Writing - review & editing.

functions in the central nervous system (CNS) ranging from memory storage to inhibiting neuronal regeneration following injury (Carulli et al., 2010; Celio et al., 1998; Chu et al., 2018; De Luca & Papa, 2016; Iwata et al., 1993; Kecskes et al., 2015; Krishnaswamy et al., 2019; Minta et al., 2019; Pizzorusso et al., 2002; Rowlands et al., 2018; Stryker et al., 2017; Suttkus et al., 2016). The PNN can restrict neuronal plasticity by acting as a physical barrier to sprouting neurons, acting as a scaffold for inhibitory molecules, as well as acting as a corral for receptors, like AMPA receptors, at the synapse (for review see (Sorg et al., 2016)). The PNN is implicated in the exit from a critical period, a period of enhanced experience-dependent plasticity found in sensory processes like audition and vision as well as cognitive processes such as learning and memory (Alberini & Travaglia, 2017; Hensch, 2005; Hou et al., 2017; Nabel & Morishita, 2013; Umemori et al., 2015).

The PNN is typically associated with the soma and proximal dendrites of neurons (Brückner et al., 2006; Dityatev et al., 2007; Fawcett et al., 2019; Giamanco et al., 2010; Matthews et al., 2002) and comprises multiple components including hyaluronic acid (HA), chondroitin sulfate proteoglycans (CSPG), hyaluronan and proteoglycan link proteins including brain associated link protein 2 (Bral2) (Bekku et al., 2012; Carulli et al., 2006; Cicanic et al., 2017; Edamatsu et al., 2018) or cartilage link protein 1 (Crtl1) (Carulli et al., 2007; Galtrey et al., 2008) and tenascin-R. Wisteria Floribunda agglutinin (WFA) or lectin is a commonly used marker for PNN because it exclusively binds to residues found in CSPG (Brückner et al., 1996; Hilbig et al., 2001; O'Connor et al., 2019). Together the components assemble into the PNN to ensheathe primarily fast-spiking neurons in many brain regions and across many species. Although interneurons, particularly inhibitory parvalbumin-positive interneurons, are more commonly found with a PNN (Baker et al., 2017; Bradshaw et al., 2018; Cabungcal et al., 2013; Guirado et al., 2014; McDonald et al., 2017; Morris & Henderson, 2000; Ohira et al., 2013; Slaker et al., 2018), there is also a subset of excitatory neurons in the CNS with a PNN (Carstens et al., 2016; Carulli et al., 2007; Morikawa et al., 2017; Seeger et al., 1994). Specifically, the deep cerebellar nuclei (DCN) are enriched with an abundance of large excitatory cells with a PNN (Bekku et al., 2012; Carbo-Gas et al., 2017; Carulli et al., 2006, 2013; de Winter et al., 2016; Edamatsu et al., 2018; Hirono et al., 2018; Mueller et al., 2016; Stamenkovic et al., 2017).

The DCN comprise the sole output of the cerebellum (Glickstein et al., 2009; Thompson & Steinmetz, 2009). The DCN, including the anterior interpositus nucleus (AIN), receive converging inputs from inhibitory Purkinje cells in the cerebellar cortex and excitatory projections from the mossy fibers originating in the pontine nucleus and the climbing fibers from the inferior olive (Steinmetz et al., 1989). As a result, the DCN are in a perfect position anatomically to integrate both the input and output pathways essential to eyeblink conditioning (EBC) and have been implicated as the crucial site of learning and memory for EBC, particularly the AIN. Although this is a contested view, lesions to the AIN do prevent acquisition, expression, and savings of the eyeblink conditioned response (CR) whereas lesions to downstream targets of the AIN involved in the output of EBC, such as the red nucleus, only eliminate the expression of the CR (Brown & Woodruff-Pak, 2011; Freeman et al., 1995; Nolan et al., 2002; Thompson & Steinmetz, 2009). Despite the abundance of the PNN in the DCN, their role in learning and memory following enzymatic disruption has not been as well studied in comparison to disruption of PNN-associated neurons in other brain

regions including the hippocampus, amygdala, and regions of the cortex (Chu et al., 2018; Hettiaratchi et al., 2019; McDonald et al., 2017; Sun et al., 2018; Xue et al., 2014).

Although there have been investigations into modifying the PNN in the DCN or cerebellar cortex, there has been little inquiry into how this affects cerebellar learning (Carbo-Gas et al., 2017; Carulli et al., 2013; Corvetti & Rossi, 2005; de Winter et al., 2016; Stamenkovic et al., 2017) or how the PNN in the DCN changes throughout development. In fact, there have been only two studies investigating PNN disruption in the DCN and the effects on EBC, and both studied mice with air puff as the unconditioned stimulus. The first study (Hirono et al., 2018) examined EBC and the synaptic electrophysiology of the large excitatory neurons in the DCN following exposure to chondroitinase ABC (ChABC), a bacterial enzyme that digests the CSPG in the PNN as evidenced by decreased WFA labelling (Bradbury et al., 2002; Brückner et al., 1998; Gogolla et al., 2009; Massey et al., 2006). The second study investigated the effects of injecting a virus expressing chondroitinase into the AIN (Carulli et al., 2020). In the Hirono et al. study, naïve male mice between P21-P23 were given ChABC infusion into the DCN and euthanized 4–6 days later to examine the electrophysiology of DCN neurons following PNN digestion in acute cerebellar slices while Carulli et al., performed in vivo recordings in adult male mice injected with a virus expressing chondroitinase. In both studies, mice that had a reduction of PNN had an enhancement of learning expressed as percent conditioned responses (% CRs) during acquisition of EBC, findings that are unlike the effects of ChABC digestion in the amygdala, which aided the removal of aversive memories following extinction without altering acquisition (Gogolla et al., 2009). The study by Carulli et al., saw similar group differences during extinction, animals with a digested PNN had lower %CRs compared to the vehicle controls, as well as group differences during acquisition. Animals in the control group in both the Hirono and Carulli studies had relatively low acquisition %CRs (around 60%) even after extensive training compared to other EBC studies using mice (Heiney et al., 2014; Koekkoek et al., 2002). There was no report of additional eyeblink parameters, such as peak latency or response amplitude, which can give a more nuanced assessment of learning effects and are perturbed in patients with diagnoses like post-traumatic stress disorder (Ayers et al., 2003). Carulli et al., found DCN neurons had a lower spontaneous firing rate after exposure to viral expression of chondroitinase (Carulli et al., 2020). Hirono et al., observed PNN disruption by infusion of ChABC in mouse cerebellar slices which showed increased amplitude of evoked inhibitory postsynaptic currents (IPSCs) as well as mini-inhibitory postsynaptic potential frequency; they also observed loss of the PNN facilitated spontaneous ISPCs (Hirono et al., 2018).

Additional studies of the role of the PNN in EBC are needed to compare differences between species. The other studies only used male mice and, as a result, were unable to assess potential sex differences. Further, cells in the DCN are excitatory neurons with a PNN, which is rather uncommon compared to the vast majority of cells with a PNN. The most common studies of the PNN investigate the relationship between the PNN and inhibitory interneurons. Only a fraction of PNN research includes excitatory cells, suggesting there is a need to look outside the interneuron population. Since EBC is not acquired well prior to P17 (Stanton et al., 1992), it is also in our interest to study how the PNN changes from the preweanling to adult in the rat DCN. The goal of this research was to

study the role of the PNN in the DCN of male and female rats by temporarily degrading the PNN with ChABC in vivo to study how ChABC infusion alters EBC in adult animals as well as in vitro application to investigate changes in the electrophysiology of the large excitatory neurons of the DCN. Our perturbations of the PNN revealed significant group differences in CR amplitude and area in addition to decreased membrane excitability in large DCN neurons.

2. Methods

2.1. Animals

Forty-three Long Evans rats (Rattus norvegicus) (male and female) between post-natal day 12 (P12) and 6 months of age were supplied by Charles River (Wilmington, MA). Twenty-six rats underwent surgery, twelve were used for ontogeny analysis, and five were slated for electrophysiological studies. Rats were housed with littermates of the same sex after weaning and were given ad libitum access to food and water and maintained on a 12 h light/dark cycle, all in accordance with the National Institute of Health guidelines. Adult rats undergoing cannulae implantation and/ or electromyogram (EMG) surgery were housed individually post-surgery. This was to prevent damage to the EMG and/ or cannulae via social grooming. All animals were socially housed until they were at least P80. All procedures were approved by the West Virginia University (WVU) Animal Care and Use Committee and the WVU Biosafety Committee.

2.2. Surgeries

Twenty-six 3-month old rats (13 F, 13 M) underwent cannula implantation in the AIN. Eight underwent bilateral cannulae implantation while eighteen had cannula implanted only in the left AIN and were also fitted with the EMG hardware for eyeblink conditioning. Sterile surgical technique was used to implant cannulae into the rat's brain at coordinates determined from the literature with reference to a stereotaxic rat brain atlas (Paxinos & Watson, 2004). Each rat was sedated with isoflurane (5% induction, 2% maintenance) with supplemental oxygen (0.5–1 L/min). The incision site (scalp) was shaved and washed three times with alternating swipes of Povidone-iodine scrub and 70% alcohol followed by application of Povidone-iodine solution after which the rat was positioned in a rodent adult stereotaxic (Kopf Model 900LS) device. Bupivacaine (max dose 2 mg/kg), a local anesthetic, was infiltrated into the scalp, which was incised with a surgical scalpel blade, to create an approximately 20-mm incision, just rostral to the eyes and just caudal to the ears. The scalp was reflected and cleaned, exposing just enough of the skull to accommodate a plastic connector for the EMG implant and up to two guide cannulae. Holes were drilled into the skull for skull screws and guide cannula implantation. Gelfoam (Capital Wholesale Drug Company, 245780) was used to stop any bleeding while drilling as the cannula drill site was over a major vessel. Each guide cannula (C317G/SPC GUIDE 23GA 38172, Plastics One, Roanoke, VA) was attached to the stereotaxic apparatus and slowly lowered at the following stereotaxic coordinates from Bregma AP: −11.5, ML: (±)3.8, DV: −5.2 from skull surface and then was secured to the skull screws with acrylic dental cement. Following surgery and excepting during infusion, dummy cannulae (C317DC/SPC DUMMY(SM) 0.010/25MM) were placed into the guide cannulae to protect the opening.

The rats assigned to EBC were next fitted with differential EMG electrodes that were implanted in the left eyelid muscle by inserting a sterile 25-gauge needle (affixed to a 1-mm empty sterile syringe) through the eyelid until the needle tip was visible on the other side as a result of the open scalp incision. The needle was then threaded with the fine wire EMG electrodes and pulled through the eyelid, leaving the recording electrode in the middle of the eyelid and the reference wire in the rostral corner of the eyelid. Where in contact around the eyelid, wires were stripped of insulation and excess wire was trimmed in an effort to prevent displacement via grooming. A bipolar stimulating electrode for delivering the electrical stimulation unconditioned stimulus was implanted subdermally, immediately caudal to the eye. The EMG recording electrode and stimulating electrode wire leads terminated on gold pins in a plastic connector, which was secured to the top of the skull, cannula, and the skull screws with acrylic dental cement. The surgical site was closed with nylon suture on both sides of the plastic connector and/ or cannulae. A non-steroidal anti-inflammatory analgesic (ketoprofen 1 mg/mL) was administered at the end of surgery and 3 mL of lactated Ringer's solution was given subcutaneously to restore any fluids lost during surgery.

2.3. Eyeblink conditioning

Rats were allowed to recover from cannula and/ or EMG surgery for four days and then underwent one session per day for five days of paired tone conditioned stimulus (CS) and periorbital electrical stimulation unconditioned stimulus (US) training followed by one session per day for three days of CS-alone extinction. The rat head plug was connected to a cable connected to a freely-rotating commutator which allowed the rat to move freely around a Coulburn Instruments modular testing cage within a sound-attenuating training chamber. The back wall of the chamber had a panel containing a speaker mounted at a 45° angle above the testing cage. The cable separated and terminated as the input to an AC/DC differential EMG amplifier (A-M Systems, Sequim, WA) and the output of a stimulus isolator (World Precision Instruments (WPI), Sarasota, FL) for shock delivery. The training chamber was lit with an LED and contained a low-light camera to allow videographic monitoring of the animal at all times. Shock was delivered by a rechargeable, constant-current stimulator (WPI, Model A365) that had been calibrated with a multimeter (WPI). LabVIEW software (National Instruments, Austin, TX) controlled the delivery of stimuli and the recording of eyelid EMG activity. Each adult rat was adapted to the enclosure without stimulus presentations for 10 min before every session. Paired delay conditioning sessions consisted of 100 trials each with 90 paired presentations of a tone CS and a periorbital electrical stimulation US as well as 10 tone-alone test trials or probes presented after every ninth paired trial to assess integrated EMG activity without a shock artifact. The tone CS consisted of a 380-ms, 88-db, 2.8-kHz pure tone. The electrical stimulation US consisted of a 100-ms, 3.0–4.0-mA, 60-Hz, ±50-volt, square-wave constant-current pulse to the periorbital region using the precalibrated stimulator. A blanking circuit in operation during the US prevented the shock from swamping the EMG signal. During the tone-shock paired trials, the CS co-terminated with the US. During acquisition, all trials were separated by an inter-trial interval averaging 30 s. To assess memory of and to extinguish responding to the tone CS, we performed CS-alone extinction beginning one day after the last paired training session. The tone CS was presented by itself for 100 trials daily on each of three consecutive days. Every 10th trial during extinction was considered a probe trial.

2.4. Behavior data analysis

Data analyses have been described previously (Schreurs et al., 2013; Smith-Bell & Schreurs, 2017; Wang et al., 2018). In brief, EMG signal was filtered (300 – 3,000-Hz), amplified, and stored (raw EMG), in addition to being rectified and integrated (20-ms time constant). Baseline activity was averaged during the first 200-ms from trial onset. If EMG activity 100-ms before CS onset was four standard deviations (SDs) or more above baseline, the trial was omitted from analysis to ensure that movement or spontaneous blinking artifacts did not artificially inflate response levels (~1% of total trials). During paired trials, we characterized unconditioned responses (URs) to the US as integrated EMG activity occurring 35-ms after the end of the US that exceeded the average baseline value by eight SDs. CRs were assessed as EMG activity that exceeded 8 SDs above the baseline during the period 80-ms after tone onset until just before US onset. This window ensured that US signal and movement or startle artifacts did not artificially inflate levels of responding. During probe trials, CRs were assessed as EMG activity beginning 80-ms after CS onset, to eliminate the potential for including alpha responses, that was eight SDs above the average baseline value during a 200-ms pre-CS period. In addition to conditioned response frequency indicated as %CRs, the amplitude of each response was calculated as the average EMG signal during the baseline period, subtracted from the maximum EMG signal during the response period. Area under the curve of the CR was obtained by summing the average heights of 2.5-ms bins of data that occurred during the CR period. Peak latency of the CR was calculated as the time when the maximum CR period height occurred (Schreurs et al., 2013; Wang et al., 2018). If an animal did not reach 70 %CRs during probe trials on at least one day of acquisition, they were excluded from behavioral analyses. This is the laboratory's standard for determining adequate levels of EBC in rats for a determination of conditioning-specific changes in unconditioned responding. Traces were made using OriginPro 2019b (OriginLab ver.9.6.5169 (Academic)).

2.5. Slice preparation and patch-clamp recordings:

Procedures identical to those previously published (Wang et al., 2018; Wang & Schreurs, 2010, 2014; Wang & Zheng, 2015) were used for slice preparation, electrophysiological recordings, and data analysis. Briefly, P24-28 rats (n = 5 rats) were anesthetized with carbon dioxide and then decapitated. Animals were selected at this age because successful recordings of DCN becomes increasingly difficult after P32 (Wang et al., 2018). After rapid brain removal, coronal cerebellar slices from the cerebellum were cut at 34°C on a vibrating slicer (LEICA VT1200S) with sucrose artificial cerebrospinal fluid (ACSF) containing (in mM) Sucrose 200, KCl 2.5, $MgCl_2$ 1.2, $CaCl_2$ 0.5, NaH_2PO_4 1.25, $NaHCO_3$ 26 and Dextrose 20, incubated for 1 h at 34 °C in 95% O_2– and 5% CO_2-saturated ACSF containing (in mM) NaCl 125, KCl 3.0, $MgSO_4$ 1.2, $CaCl_2$ 2.0, NaH_2PO_4 1.2, $NaHCO_3$ 26 and Dextrose 10. After postslicing recovery, slices were maintained at room temperature until electrophysiological recording. Vertical vibration of the blade was manually adjusted with a Vibrocheck device (Leica) before slice preparation and set to 0 μM.

A slice was placed in a modified recording chamber containing ACSF. DCN neurons were identified morphologically through a 40X water immersion objective using DIC-IR optics (Olympus BX50WI, Dulles, VA). Whole-cell patch-clamp recordings were performed using

an Axon MultiClamp 700B on cells with diameters of 15–20 μM in the interpositus and the medial portion of the lateral nucleus. These neurons are regarded as large glutamatergic projection neurons (Aizenman et al., 2003; Huang & Uusisaari, 2013). Generally, recordings were performed in 2–3 cells from DCN slices per rat after the slices were exposed to ChABC or Vehicle in the medium. Patch pipettes made from borosilicate glass (catalog #: BF150-86–10; 1.5 mm OD, 0.86 mm ID; Sutter Instrument Company, Novato, CA) were pulled with a P97 Brown-Flaming micropipette puller (Sutter Instrument Company, Novato, CA). The final resistances of pipettes filled with the internal solution [containing (in mM) potassium gluconate ($C_6H_{11}O_7K$) 140, $MgCl_2 \cdot 6H_2O$ 4.6, HEPES 10, EGTA 10, Na_2ATP 4.0, pH 7.3 (KOH)] were between 5 and 8 MΩ. Data were low-pass filtered at 2 kHz and acquired at 20 kHz. Membrane properties were measured when the neuron had stabilized for 5 min after the whole-cell configuration was achieved. Quantitative analysis included resting membrane potential measured directly upon breakthrough in whole-cell configuration, input resistance based on membrane potential changes to depolarizing current injections immediately after whole cell configuration, action potential (AP) threshold, current required for eliciting the first AP, half-width of elicited AP (APD50) including rising and falling phases, amplitude of elicited AP, the number of elicited APs, latency to the first AP elicited by a 250-ms duration depolarizing current injection, peak amplitude of the afterhyperpolarization (AHP), interval between first and second evoked action potentials (S1S2 interval), current required for hyperpolarization-induced rebound spikes, and the properties of rebound spikes. Recordings were only accepted if the resistance of initial seal formations were greater than 1 GΩ and rejected if their output was unstable or series resistance changed by more than 20%. To obtain an accurate measurement of neuronal excitability independent of membrane potential changes, continuous direct current was applied through the recording electrode to hold the cell at a − 70 mV baseline. All recordings were made at room temperature. All electrophysiological data were recorded online using Clampex 10.0 software (Molecular Devices, LLC.). Standard off-line analyses were conducted using Clampfit 10.0 (Molecular Devices, LLC.).

2.6. ChABC degradation of PNN

2.6.1. ChABC in vivo—A 0.5 μL solution containing either ChABC (0.01U/μg/side/0.5 μL) or vehicle (0.1 M PBS) was infused into the left AIN. We chose to perform a unilateral infusion because a number of studies have demonstrated that the ipsilateral DCN is largely responsible for the CR when testing the ipsilateral eye (Bracha et al., 1997; Campolattaro & Freeman, 2009; Freeman et al., 1995; Gerwig et al., 2006; Miller et al., 2003). Infusate was injected using a microinfusion pump at a rate 0.5 μL/ minute and the infusion cannula (C317I/SPC, INTERNAL 30GA, Plastics One, Roanoke, VA) was kept in place for another 2 min to allow diffusion into the cerebellar tissue. Afterwards, the infusion cannula was removed and replaced with a dummy cannula for the remainder of the experiment. Immediately following removal, sterile water was run through the infusion cannulae to ensure none had clogged. Rats were returned to their home cage for 4 days following ChABC infusion to allow for PNN digestion. The dosage and timing of ChABC infusion and timing of PNN digestion was derived from the literature (Gogolla et al., 2009; Hirono et al., 2018; Xue et al., 2014). Littermates were randomly assigned to the ChABC or vehicle

group during surgery and attempts were made to ensure equal numbers of males and females were included in each group.

2.6.2. ChABC in vitro incubation—A stock solution of 10U/mL of ChABC was made according to manufacturer specifications. During slice incubation, of ACSF for a final ChABC concentration of 0.25U/mL or 250 μL of the 0.01% BSA vehicle solution was added into ACSF as a vehicle. Tissue slices were cut at 350 μm and incubated in either ChABC or vehicle medium. A pilot experiment was done by incubating brain slices with either ChABC or vehicle medium for 4, 5, 6, and 8 h, respectively, in order to determine the optimal ChABC incubation duration for PNN disruption. Our data - indicated an incubation time of 8 h was best-suited for ChABC digestion and this time was used for electrophysiological recordings as well as processing of in vitro tissue.

2.7. Tissue processing

In vitro electrophysiology tissue slices were transferred to 4% paraformaldehyde for 5 days then transferred to 30% sucrose for cryoprotection until they sank. Following cryoprotection, tissue was resectioned on a freezing microtome (HM 450 sliding microtome, Microm of Thermo Fisher Scientific) at 40 μm. Tissue was either mounted onto 3% gelatin slides or placed into cryoprotection in −20 °C.

Rats used for the ontogeny analysis, in vivo ChABC degradation, and/ or eyeblink conditioning were given a subcutaneous injection of ketamine hydrochloride (80 mg/kg) mixed with xylazine (8.0 mg/kg). Animals were perfused transcardially with 0.9% saline (pH 7.4 at room temperature) followed by 4% paraformaldehyde. Brains were collected and placed in fixative until ready for processing. Brains were transferred to 30% sucrose for cryoprotection until they sank, then 40-μm sections were cut on a freezing microtome. Tissue was either mounted onto 3% gelatin slides or placed into cryoprotection at −20 °C.

2.8. PNN immunofluorescence

Mounted sections from both the in vitro and in vivo experiments were washed in 0.1 M phosphate buffered saline (PBS) − 1% Tween then blocked for 2 h with 5% normal donkey serum or normal goat serum and 3% BSA before being incubated with primary antibodies overnight at 4 °C. Following washing in 0.1MPBS, sections were incubated in secondary antibody and 1% blocking solution for 4 h. After completing the secondary antibody reaction, sections were washed again in 0.1 M PBS. Following the final wash, sections were cover-slipped with DAPI Fluoromount-G mounting media and #1.5 coverslips (Fisher Scientific). Manufacturers' information for primary antibodies, secondary antibodies, and sera can be found in Table 1.

2.9. Image acquisition

Neuronal and PNN immunofluorescent reactivity in the rat cerebellum was visualized using a confocal laser-scanning microscope (Zeiss LSM 710; Carl Zeiss International). Images were acquired using 405, 488, 546, and 633 nm lasers, sequential multichannel line scan, and with filters set manually to detect the spectral peak of each fluorophore. Cells were imaged at 20X (NA 0.4) and 63X oil-immersion (NA 1.4) objectives. Raw images were

exported to Zen Lite 2009 and Adobe Photoshop CC 2017 to make minor adjustments to the brightness and contrast. Raw images were also exported to FIJI (ImageJ, NIH) to determine the percentage of WFA positive (WFA+) neurons (neurons with a PNN) at multiple time points of development (P12, P16, P18, P30, 3 months, and 6 months) and following either in vitro exposure or in vivo infusion of ChABC or vehicle solution. For PNN analysis, an average of 6 sections per animal were imaged; images were analyzed between the following coordinates (Bregma: 11.52 mm, Interaural: −2.52 mm and Bregma: 10.68 mm, Interaural: −1.68 mm). Each section was imaged bilaterally with the imager blind to the side. In FIJI, the channels were separated in order to compare the number of microtubule-associated protein 2-positive (MAP2+) cells to the WFA+ cells to obtain a normalized count for each image. MAP2 is a protein found in both developing and adult neurons and can be used as a biomarker for neurons (Dehmelt & Halpain, 2004; Kindler & Garner, 1994; Matus et al., 1990; Tucker et al., 1988). Once channels were separated, a background subtraction was performed to further distinguish WFA+ or MAP2+ cells. Images were thresholded to produce binary images and then particle analysis was used to generate a count of WFA+ or MAP2+ cells. Counts were made every ten slices and the average number of WFA+ cells divided by the average number of MAP2+ cells and then multiplied by 100 to generate a percentage of PNN+ neurons.

2.10. Statistical analysis

Data are presented as mean and ± SEM. One-way ANOVA, two-way ANOVA, and paired and unpaired t-tests were calculated in IBM SPSS Statistics (Ver.26.00.0; IBM Corp.) with $p < 0.05$ as the criterion for significance.

3. Results

3.1. Ontogenetic differences in the AIN

We examined WFA reactivity of MAP2+ cells in the AIN at six time points (P12, P16, P18, P30, 3 months, and 6 months) (Fig. 1) and differences were found as a result of age, [$F(5, 37) = 47.75$, $p < .000$]. Fig. 1 shows that at P12 and P16 little WFA reactivity was seen but by P18 and P32, there was a dense PNN surrounding the cell body as indicated by high WFA reactivity. P12 and P16 rats had a lower percentage of PNN+ neurons compared to rats at P18, P30, 3 months, and 6 months. Fig. 1 also shows higher-resolution images of WFA reactivity at P12, P30, and 3 months. There were no significant changes in the percentage of PNN+ neurons in the AIN from P18 to 6 months.

3.2. PNN digestion in vivo alters eyeblink conditioning

3.2.1. In vivo PNN digestion—We examined PNN function by performing bilateral cannulae implants into the AIN of adult rats with one side being infused with ChABC and the other with vehicle. The PNN in the AIN on the side that received the enzymatic infusion was found to be digested 4 days post-infusion (42.38 ± 5.24%) compared to the side receiving vehicle (68.78 ± 5.14%), $p < .000$. Although other brain areas have significant PNN digestion that occurs more quickly following ChABC infusion (Gogolla et al., 2009; Xue et al., 2014), the DCN requires an extended time to achieve PNN digestion at similar concentrations (Hirono et al., 2018). We found that this level/amount of degradation to the

PNN was present for approximately one month following infusion of ChABC (data not shown). The reassembly of the PNN after a month demonstrated that ChABC infusion into the DCN was a temporary digestion of the PNN (Brückner et al., 1998).

Rats were removed from the study if their EMG signal-to-noise ratio was so small it was impossible to distinguish their responses from baseline activity. Eighteen adult male and female rats (at least P90) were included in the behavioral data analysis after five sessions of paired EBC (n = 9 ChABC (6F,3M), n = 9 vehicle (5F,4M) on final acquisition session) and up to three sessions of tone-only extinction (n = 7 ChABC (4F,3M), n = 8 vehicle (4F,4M) on final extinction session) following infusion of ChABC or PBS vehicle into the AIN. These numbers decreased as the experiment progressed because grooming disrupted the EMG signal over the course of the experiment by displacing the EMG wires in the eyelid. Even if an animal had poor EMG signal and their behavioral results could not be analyzed for that particular day, they were still placed in the chamber and exposed to the stimuli and brain tissue was stained and imaged to confirm ChABC digestion. Fig. 2 shows ChABC was capable of successfully digesting the PNN; we found that adult rats receiving infusion of ChABC prior to EBC had fewer MAP2+ neurons associated with the PNN (55.1 ± 3.2%) compared to vehicle who had EBC (86.4 ± 2.5%), $p < .000$.

3.2.2. EBC acquisition—Fig. 3 shows a timeline for the behavioral experiments. Fig. 4 shows there was an increase in %CRs for both groups across sessions, [$F(4,77) = 5.82$, $p < .000$], with Session 1 (S1) having lower %CRs than S3 ($p = .001$), S4 ($p = .016$), and S5 ($p = .001$) but there were no overall differences in %CRs between groups.

There were several changes to the parameters of CRs during paired EBC, which are important tools for measuring an animal's ability to learn EBC. As expected from previous research (Burhans et al., 2013; Schreurs et al., 2013), Fig. 5 shows session differences in CR amplitude were observed [$F(4,73) = 4.68$, $p = .002$], with S1 having lower amplitudes than S4 ($p = .008$) and S5 ($p = .004$). There was also a session by group interaction for CR amplitude [$F(9, 73) = 3.43$, $p = .001$]. Rats that received ChABC had lower CR amplitudes during the final session (S5) compared to vehicle animals (Fig. 5). Representative traces of individual probe trials are shown for a ChABC-infused subject (red) and a Vehicle-infused subject (blue) in the in Fig. 5B.

As expected with robust classical conditioning of the EBC, there were session differences in the CR area, seen in Fig. 6, [$F(4,73) = 5.28$, $p = .001$] which were smaller on S1 compared to S4 ($p = .008$) and S5 ($p = .003$). More importantly, the ChABC group had reduced CR area compared to the vehicle group, [$F(1, 73) = 7.72$, $p = .007$]. ChABC infused rats had smaller CR area compared to vehicle animals on both the first (2.74 ± 0.35 AU in vehicle, 0.000 ± 0.26 AU in ChABC, $p = 0.02$) and final session of acquisition (4.75 ± 0.62 AU in vehicle, 3.01 ± 0.37 AU in ChABC, $p = 0.03$) (Fig. 6). Representative individual traces on probe trials (ChABC in red, vehicle in blue) for two sessions of acquisition, corroborate these averaged data (Fig. 6B). The changes observed in amplitude and area suggest that digestion of the PNN diminished the size of the conditioned response.

Following ChABC or vehicle infusion, there were session differences associated with peak eyeblink latency, [F (4, 74) = 8.17, p < .000] with the eyeblink peak response occurring earlier on S3 (p = 0.03), S4 (p < .000), and S5 (p < .000) compared to S1 (Smith-Bell et al., 2012). The eyeblink response grew faster by the end of acquisition. There were no significant group differences in the peak latency of the CR (F < 1).

No significant differences were found in any of the UR measures between the animals infused with ChABC versus vehicle suggesting that there were no effects of ChABC on the motor output pathway (F's < 1).

3.2.3. EBC extinction—Fig. 4 shows the %CRs during the three extinction sessions. Analysis yielded only session differences, [F (2, 43) = 3.36, p = .044], with the final extinction session (E3) having lower %CRs than the first extinction session (E1) (Fig. 4B). There were no significant differences in any of the other conditioned response parameters investigated during extinction (F's < 1).

3.2.4. Sex differences—There were some effects of sex on %CRs during EBC seen in Fig. 7. The vehicle group exhibited sex differences with female rats having marginally higher %CRs than males during some acquisition sessions, [F (1, 54) = 3.91, p = .053] (Fig. 7A). These sex differences were not evident in the ChABC group (F < 1). In the vehicle group, sex differences were found in %CRs on post-probe trials, the paired trials that immediately followed the tone-alone probes that were presented every ten trials during acquisition, [F (1,32) = 9.66, p = .004], with female rats having higher %CRs on the next reinforced trial that followed the probe trial compared to their male counterparts. Again, the ChABC group did not exhibit these sex differences (Fig. 7B).

Lastly, Fig. 8 shows an effect of sex on CR area. This was observed for both the vehicle group, [F (1, 48) = 27.63, p < .001] and the ChABC group, [F (1,44) = 7.72, p = .008] during acquisition. The female rats in both groups had a larger CR area than the males.

3.3. In vitro PNN digestion alters the electrophysiological properties of neurons in the AIN

0.25 U/mL of ChABC successfully digested the PNN in DCN slices. Fig. 9 shows AIN tissue that was exposed to ChABC in the medium had lower WFA reactivity compared to tissue placed in the vehicle medium. An unpaired *t*-test confirmed that the AIN tissue exposed to ChABC had a lower percentage of WFA+ neurons (41.98 ± 4.75) compared to the vehicle group (98.71 ± 0.38), p < .000. Table 2 depicts which membrane properties of neurons in the rat AIN were altered by exposure to ChABC.

Fig. 10 shows neurons exposed to ChABC required a larger current (0.04 ± 0.01nA) to fire an action potential (AP) compared to cells in the vehicle group (0.02 ± 0.01nA), p = 0.009, (Fig. 10A) and had a longer latency to evoke an AP (45.99 ± 9.51 ms) compared to cells from vehicle animals (20.27 ± 4.19 ms), p = 0.03 (Fig. 10B). AIN excitatory neurons also showed a prolonged inter-spike interval (S1S2) when exposed to ChABC (31.2 ± 5.0 ms) compared to the neurons in the vehicle media (17.83 ± 3.14 ms), p = 0.04 (Fig. 10C). Fig. 11 shows ChABC-exposed neurons had a larger afterhyperpolarization (AHP) amplitude

(−12.46 ± 1.12 mV) compared to vehicle cells (−8.88 ± 1.36 mV), p = 0.04 (Fig. 11A). The voltage to reach AP threshold was lower following ChABC exposure (−42.70 ± 0.94 mV) compared to the vehicle group neurons (−47.90 ± 1.84 mV), p = .008 (Fig. 11B). Interestingly, there were no differences in the membrane potential (−46.93 ± 0.82 mV and −46.4 0 ± 0.69 mV) or input resistance (132.95 ± 15.6 MΩ and 124.03 ± 1.07 MΩ) of neurons exposed to ChABC compared to vehicle. These results suggest that digestion of PNN with ChABC in acute AIN slices decreased the intrinsic excitability of large excitatory neurons without affecting other membrane properties.

The electrophysiological properties of rebound spikes (RD) are summarized in Table 3 and seen in Fig. 12. Neurons in the DCN slices exposed to ChABC required a larger current for evoked rebound spikes (−0.59 ± 0.11nA) compared to those exposed to the vehicle media (−0.29 ± 0.01nA), p = 0.03 (Fig. 12A). In addition, there were fewer evoked RD in DCN neurons exposed to ChABC (4.63 ± 0.9) versus those exposed to the vehicle solution (10.3 ± 0.74), p = 0.0003 (Fig. 12B). Increased rebound firing in the DCN is associated with higher likelihood of inducing changes responsible for cerebellar learning (Person & Raman, 2012; Pugh & Raman, 2006; Zheng & Raman, 2010, 2011). Taken together, it is likely that ChABC exposure removed the surrounding PNN resulting in modified the intrinsic membrane properties of the large excitatory neurons within the DCN.

4. Discussion

The principal findings of the present experiment were: (1) ChABC was able to digest PNNs in the rat DCN that emerge almost fully formed at P18; (2) In vivo ChABC digestion of the PNNs in the DCN had deleterious effects on eyeblink conditioning particularly on the size of the conditioned response without affecting the unconditioned response; (3) Exposure to ChABC in vitro profoundly affected membrane properties of large, excitatory neurons in the DCN significantly reducing membrane excitability which has been shown to play a role in eyeblink conditioning.

Our investigation of PNN development in the DCN adds to the current literature that describes the presence of the PNN in this region for adults and at only a few early timepoints. Rats and other animals younger than P18 have difficulty acquiring and retaining EBC and this may be the result of an underdeveloped PNN. Even at P17-P18, rats do not learn EBC with an auditory CS as quickly or as well as they do at P24 (Stanton et al., 1992). This difficulty in training rats younger than P17-18 with an auditory CS may also be due in part to an immature auditory sensory pathway (Freeman & Rabinak, 2005), since training is possible if the CS is a somatosensory stimulus like shock (Schreurs et al., 2013) or vibration (Goldsberry et al., 2014), because unlike auditory pathways, the somatosensory pathways mature prenatally. Training rats as young as P12 is possible if the pontine nuclei are directly stimulated as the CS (Freeman & Rabinak, 2005). The PNN could also be implicated in age-related differences in extinction of EBC. In a study comparing P17 and P24 rats, direct stimulation of the middle cerebellar peduncle as a CS paired with a 25-ms, 3.0-mA (range 2.5–3.5 mA) periorbital stimulation US was used to overcome the immature auditory system so that both ages had strong CRs at the end of acquisition. Even with strong CRs, results showed that P17 animals had a faster rate of extinction compared to P24 animals. P24

animals also had a faster rate of reacquisition following extinction, suggesting that the original memory was better stabilized in P24 rats (Brown & Freeman, 2014). Although P24 rats are still within their critical period, it is possible that they have more PNN+ cells than preweanlings aged P17, suggesting they are more likely to stabilize the associations learned from EBC. Even rats at P24, a "periweanling" age, still diverge in their conditioned behavior compared to adults at P60-P90 (Brown & Freeman, 2016). The authors of that 2016 study found that there were unremarkable differences between the periweanlings and adult rats in acquisition and extinction following 1, 7, or 28 days after conditioning took place. However, when they reexposed periweanlings to the CS-US pairings 29 days following conditioning, they required more training to achieve the high levels of CRs observed during their initial training, suggesting that some memory instability persists in periweanling rats. Together, the behavioral results found by Brown and Freeman as well as our ontogenetic analysis of the PNN and behavior demonstrate that there are age-related differences in an animal's ability to learn EBC. These developmental differences may be dependent on the presence of the PNN in the DCN as well as other brainstem structures related to EBC. Further examination of the changes to the PNN following EBC at various ontogenetic stages would prove a logical next step.

ChABC infusion 4 days prior to five sessions of EBC and three sessions of EBC extinction was sufficient to significantly reduce the PNN as well as loose ECM. Exposure to EBC and other stimuli may also remodel the PNN as a result of endogenous enzymatic activity related to learning or changes in the cage environment as observed by others (Carulli et al., 2020; Stamenkovic et al., 2017). Both vehicle and ChABC groups reached our predefined conditioning criterion (70% CR) by S3. We may have missed subtle conditioning differences when comparing between training sessions due to the intensity of our stimuli and the consequent rapid level of learning.

To assess more subtle conditioning differences, we investigated within the acquisition and extinction sessions by assessing %CRs in 10-trial blocks (Smith-Bell & Schreurs, 2017). Although all rats acquired equal levels of %CRs during the first four sessions, group differences emerged during the last session (S5), with ChABC-treated subjects having lower %CRs than vehicle-treated controls. The nature of this difference was explored by examining the final 10-trial block during one session versus the next session's first 10-trial block (Smith-Bell & Schreurs, 2017). We found a group difference on the final 10-trial block of S4 and the first 10-trial block of the final session of acquisition (S5). Rats in the vehicle group may have had higher %CRs compared to those that had been infused with ChABC. This evidence suggests ChABC infused rats were unable to successfully consolidate their memories as well as vehicle rats. This more in-depth analysis within each extinction session revealed that on E1 there was a group by 10-trial block interaction. ChABC-infused rats had lower %CRs, while there were differences between the 10-trial blocks, withT1-10 having higher %CRs than the remaining 10-trial blocks. We also found differences within 10-trial blocks when comparing ChABC and vehicle controls on the second extinction session (E2). Although we followed previously published timelines with ChABC infused degradation in the DCN, additional time may have been needed to achieve the maximum PNN digestion. However, to ensure viable signal quality from the EMG, we

had to begin training as rapidly as possible while allowing ChABC enough time to enzymatically alter the PNN.

Nevertheless, we did find conditioning parameters that were significantly different between the two groups. Animals with a digested PNN had conditioned eyeblink responses with smaller amplitudes and with smaller areas compared to vehicle rats. Indeed, the amplitude of conditioned eyeblink responses increased in size in vehicle animals from the second session to the final session while ChABC animal amplitude plateaued by the second session. We observed fairly consistent differences in the CR area which can be interpreted as a measure of CR strength. This difference could be an effect of ChABC on the CR output pathway. The smaller amplitude and area of the conditioned eyeblink response in rats with degraded PNN in the AIN may be a result of the decreased intrinsic membrane excitability and altered inhibitory connections onto the DCN. The study by Carulli et al., found reorganization of the inhibitory and excitatory connections of DCN neurons following PNN digestion (Carulli et al., 2020). One reason we did not observe differences in conditioning levels could not only be due to the extent of PNN digestion but also the fact that the DCN neurons remained functional, unlike with the extensive damage observed following cerebellar lesions. Interestingly, other studies have observed impairments of CR amplitude without drastic changes to the CR acquisition following DCN lesions (Perciavalle et al., 2013; Welsh, 1992) while some have used CR amplitude as the measure of cerebellar learning (Kreider & Mauk, 2010). Since we did not find any differences between the two groups in responding to the US, it is highly unlikely that the observed differences resulted from alterations in the motor performance of ChABC animals. Instead, ChABC-infused rats may not have had well-stabilized associations of the tone-shock pairings with a reduced PNN leading to responses that were decreased in both amplitude and area. Other studies that investigated PNN digestion in the mouse cerebellum and its effect on EBC chose to train mice using air puff as the US (Carulli et al., 2020; Hirono et al., 2018). The lower salience of an air puff US and the lower rate of learning in those studies may have allowed for differences in % CRs between ChABC and vehicle-infused groups to emerge between sessions on acquisition. The authors did not investigate parameters of the eyeblink response other than percent CR.

Lastly, we observed significant sex differences during EBC. The females in both the Vehicle and ChABC groups had larger CR areas than their male counterparts during acquisition of EBC. Females in the vehicle group had marginally higher percent CRs during conditioning and significantly higher post-probe percent CRs compared to males in the group suggesting they may have formed stronger associations compared to the males. This has been observed in delay and trace conditioning with female animals having higher %CRs (Dalla et al., 2009; Dalla & Shors, 2009; Leuner et al., 2004; Waddell et al., 2010). In comparison, females and males in the ChABC group performed at similar levels. These results confirm that sex is an important biological variable in learning and memory (Bangasser & Shors, 2007; Chow et al., 2013; Shors & Miesegaes, 2002) and may indicate the PNN's role (if any) in disorders or diseases that seem to impact one sex more than the other. These data suggest that researchers studying the PNN should consider including animals from both sexes.

The observed changes in vitro, may help explain the observed behavioral changes seen following ChABC infusion to the AIN. We observed that degradation of the PNN in vitro

leads to changes in membrane properties of the large excitatory neurons in the DCN. Slices exposed to ChABC had a significantly diminished level of PNN in comparison to slices exposed to the vehicle. The reduction of the PNN decreased the intrinsic membrane excitability of these neurons based on an observed prolonged latency for evoked AP, an extended S1S2 interval, evoked AP needing a larger current, as well as a relatively larger AHP amplitude without altering membrane voltage, input resistance, or amplitude. The ChABC-induced digestion of the PNN altered the membrane properties of DCN neurons modifying the way these cells behaved. In agreement with these results, there are other reports of decreased excitability following PNN removal (Balmer, 2016; Chu et al., 2018). However, others have found increased excitability after ChABC exposure (Dityatev et al., 2007; Hayani et al., 2018). We have observed that eyeblink conditioning is correlated to increased excitability of DCN neurons (Wang et al., 2018; Schreurs, 2019) and others found similar results in the hippocampus (McEchron et al., 2003; Moyer et al., 1996, 2000; Oh & Disterhoft, 2015). We would then expect to observe a decrease in the conditioning of animals exposed to ChABC, since the digestion of the PNN resulted in decreased excitability. These differences may have to do with the location, type of neuron that is being studied, composition of CSPG in PNN, and level of PNN degradation. Although we did not find any significant differences in the PNN in the DCN post P18, our electrophysiology recordings were made when these animals were still in their periweanling stage, suggesting that there may be differences in the effects of PNN degradation on DCN neurons between animals at this age and adults of 3 months or older. These recordings were made in periweanlings because it is difficult to successfully patch and record neurons in the DCN post P32 (Wang et al., 2018). In the future, we are interested in discerning if the changes we observed following in vitro digestion are also found when breaking down the PNN via ChABC infusion in vivo and performing electrophysiological experiments four days post infusion.

5. Conclusion

In summary, we found that PNN levels were less prevalent at P12-P16 but increased until P18 and remained stable from this point onward. We observed that digesting the PNN in the rat DCN altered several parameters of EBC and decreased the intrinsic excitability of the PNN+ neurons. These results add to the growing body of work studying the PNN and its function in the CNS.

Acknowledgements:

National Institute of General Medical Sciences grant T32 GM081741 and Eunice Kennedy Shriver National Institute of Child & Human development grant HD099338 for funding support. The content is solely the responsibility of the authors and does not necessarily represent the official views of the National Institutes of Health.

References

Aizenman CD, Huang EJ, & Linden DJ (2003). Morphological correlates of intrinsic electrical excitability in neurons of the deep cerebellar nuclei. Journal of Neurophysiology, 89(4), 1738–1747. 10.1152/jn.01043.2002. [PubMed: 12686564]

Alberini CM, & Travaglia A (2017). Infantile Amnesia: A Critical Period of Learning to Learn and Remember. Journal of Neuroscience, 37(24), 5783–5795. 10.1523/JNEUROSCI.0324-17.2017. [PubMed: 28615475]

Araque A, Parpura V, Sanzgiri RP, & Haydon PG (1999). Tripartite synapses: Glia, the unacknowledged partner. Trends in Neurosciences, 22(5), 208–215. 10.1016/S0166-2236(98)01349-6. [PubMed: 10322493]

Ayers ED, White J, & Powell DA (2003). Pavlovian Eyeblink Conditioning in Combat Veterans With and Without Post-Traumatic Stress Disorder. Integrative Physiological & Behavioral Science, 38(3), 230–247. [PubMed: 15070085]

Baker KD, Gray AR, & Richardson R (2017). The development of perineuronal nets around parvalbumin gabaergic neurons in the medial prefrontal cortex and basolateral amygdala of rats. Behavioral Neuroscience, 131(4), 289–303. 10.1037/bne0000203. [PubMed: 28714715]

Balmer TS (2016). Perineuronal Nets Enhance the Excitability of Fast-Spiking Neurons. ENeuro, 3(4), ENEURO.0112-16.2016. 10.1523/ENEURO.0112-16.2016.

Bangasser DA, & Shors TJ (2007). The hippocampus is necessary for enhancements and impairments of learning following stress. Nature Neuroscience, 10(11), 1401–1403. 10.1038/nn1973. [PubMed: 17906620]

Bekku Y, Saito M, Moser M, Fuchigami M, Maehara A, Nakayama M, … Oohashi T (2012). Bral2 is indispensable for the proper localization of brevican and the structural integrity of the perineuronal net in the brainstem and cerebellum. The Journal of Comparative Neurology, 520(8), 1721–1736. 10.1002/cne.23009. [PubMed: 22121037]

Bracha V, Zhao L, Wunderlich DA, Morrissy SJ, & Bloedel JR (1997). Patients with cerebellar lesions cannot acquire but are able to retain conditioned eyeblink reflexes. Brain, 120(8), 1401–1413. 10.1093/brain/120.8.1401. [PubMed: 9278630]

Bradbury EJ, Moon LDF, Popat RJ, King VR, Bennett GS, Patel PN, … McMahon SB (2002). Chondroitinase ABC promotes functional recovery after spinal cord injury. Nature, 416(6881), 636–640. 10.1038/416636a. [PubMed: 11948352]

Bradshaw KP, Velez DXF, Habeeb M, & Gandhi SP (2018). Precocious deposition of perineuronal nets on Parvalbumin inhibitory neurons transplanted into adult visual cortex. Scientific Reports, 8(1), 7480. 10.1038/s41598-018-25735-8. [PubMed: 29748633]

Brown KL, & Freeman JH (2014). Extinction, reacquisition, and rapid forgetting of eyeblink conditioning in developing rats. Learning & Memory (Cold Spring Harbor, N. Y.), 21(12), 696–708. 10.1101/lm.036103.114.

Brown KL, & Freeman JH (2016). Retention of eyeblink conditioning in periweanling and adult rats. Developmental Psychobiology, 58(8), 1055–1065. 10.1002/dev.21439. [PubMed: 27279383]

Brown KL, & Woodruff-Pak DS (2011). Eyeblink Conditioning in Animal Models and Humans. In Raber J (Ed.), Animal Models of Behavioral Analysis (Vol. 50, pp. 1–27). Humana Press Inc.

Brückner G, Brauer K, Härtig W, Wolff JR, Rickmann MJ, Derouiche A, … Reichenbach A (1993). Perineuronal nets provide a polyanionic, glia-associated form of microenvironment around certain neurons in many parts of the rat brain. Glia, 8(3), 183–200. 10.1002/glia.440080306. [PubMed: 7693589]

Brückner G, Bringmann A, Härtig W, Köppe G, Delpech B, & Brauer K (1998). Acute and long-lasting changes in extracellular-matrix chondroitin-sulphate proteoglycans induced by injection of chondroitinase ABC in the adult rat brain. Experimental Brain Research, 121(3), 300–310. 10.1007/s002210050463. [PubMed: 9746136]

Brückner G, Bringmann A, Köppe G, Härtig W, & Brauer K (1996). In vivo and in vitro labelling of perineuronal nets in rat brain. Brain Research, 720(1), 84–92. 10.1016/0006-8993(96)00152-7. [PubMed: 8782900]

Brückner G, Szeöke S, Pavlica S, Grosche J, & Kacza J (2006). Axon initial segment ensheathed by extracellular matrix in perineuronal nets. Neuroscience, 138(2), 365–375. 10.1016/j.neuroscience.2005.11.068. [PubMed: 16427210]

Burhans LB, Smith-Bell CA, & Schreurs BG (2013). Subacute fluoxetine enhances conditioned responding and conditioning-specific reflex modification of the rabbit nictitating membrane

response: Implications for drug treatment with selective serotonin reuptake inhibitors. Behavioural Pharmacology, 24(1), 55–64. 10.1097/FBP.0b013e32835d528e. [PubMed: 23263485]

Cabungcal J-H, Steullet P, Morishita H, Kraftsik R, Cuenod M, Hensch TK, & Do KQ (2013). Perineuronal nets protect fast-spiking interneurons against oxidative stress. Proceedings of the National Academy of Sciences of the United States of America, 110(22), 9130–9135. 10.1073/pnas.1300454110. [PubMed: 23671099]

Campolattaro MM, & Freeman JH (2009). An Examination of Bilateral Eyeblink Conditioning in Rats. Behavioral Neuroscience, 123(6), 1346–1352. 10.1037/a0017314. [PubMed: 20001118]

Carbo-Gas M, Moreno-Rius J, Guarque-Chabrera J, Vazquez-Sanroman D, Gil-Miravet I, Carulli D, … Miquel M (2017). Cerebellar perineuronal nets in cocaine-induced pavlovian memory: Site matters. Neuropharmacology, 125 (Supplement C), 166–180. 10.1016/j.neuropharm.2017.07.009. [PubMed: 28712684]

Carstens KE, Phillips ML, Pozzo-Miller L, Weinberg RJ, & Dudek SM (2016). Perineuronal Nets Suppress Plasticity of Excitatory Synapses on CA2 Pyramidal Neurons. Journal of Neuroscience, 36(23), 6312–6320. 10.1523/JNEUROSCI.0245-16.2016. [PubMed: 27277807]

Carulli D, Broersen R, de Winter F, Muir EM, Mešković M, de Waal M, de Vries S, Boele H-J, Canto CB, De Zeeuw CI, & Verhaagen J (2020). Cerebellar plasticity and associative memories are controlled by perineuronal nets. Proceedings of the National Academy of Sciences of the United States of America. 10.1073/pnas.1916163117.

Carulli D, Foscarin S, Faralli A, Pajaj E, & Rossi F (2013). Modulation of semaphorin3A in perineuronal nets during structural plasticity in the adult cerebellum. Molecular and Cellular Neurosciences, 57, 10–22. 10.1016/j.mcn.2013.08.003. [PubMed: 23999154]

Carulli D, Pizzorusso T, Kwok JCF, Putignano E, Poli A, Forostyak S, … Fawcett JW (2010). Animals lacking link protein have attenuated perineuronal nets and persistent plasticity. Brain, 133(8), 2331–2347. 10.1093/brain/awq145. [PubMed: 20566484]

Carulli D, Rhodes KE, Brown DJ, Bonnert TP, Pollack SJ, Oliver K, … Fawcett JW (2006). Composition of perineuronal nets in the adult rat cerebellum and the cellular origin of their components. The Journal of Comparative Neurology, 494(4), 559–577. 10.1002/cne.20822. [PubMed: 16374793]

Carulli D, Rhodes KE, & Fawcett JW (2007). Upregulation of aggrecan, link protein 1, and hyaluronan synthases during formation of perineuronal nets in the rat cerebellum. The Journal of Comparative Neurology, 501(1), 83–94. 10.1002/cne.21231. [PubMed: 17206619]

Celio MR, Spreafico R, Biasi SD, & Vitellaro-Zuccarello L (1998). Perineuronal nets: Past and present. Trends in Neurosciences, 21(12), 510–515. 10.1016/S0166-2236(98)01298-3. [PubMed: 9881847]

Chow C, Epp JR, Lieblich SE, Barha CK, & Galea LAM (2013). Sex differences in neurogenesis and activation of new neurons in response to spatial learning and memory. Psychoneuroendocrinology, 38(8), 1236–1250. 10.1016/j.psyneuen.2012.11.007. [PubMed: 23219473]

Chu P, Abraham R, Budhu K, Khan U, De Marco Garcia N, & Brumberg JC (2018). The Impact of Perineuronal Net Digestion using Chondroitinase ABC on the Intrinsic Physiology of Cortical Neurons. Neuroscience. 10.1016/j.neuroscience.2018.07.004.

Cicanic M, Edamatsu M, Bekku Y, Vorisek I, Oohashi T, & Vargova L (2017). A deficiency of the link protein Bral2 affects the size of the extracellular space in the thalamus of aged mice. Journal of Neuroscience Research. 10.1002/jnr.24136.

Cope EC, & Gould E (2019). Adult Neurogenesis, Glia, and the Extracellular Matrix. Cell Stem Cell, 24(5), 690–705. 10.1016/j.stem.2019.03.023. [PubMed: 31051133]

Corvetti L, & Rossi F (2005). Degradation of chondroitin sulfate proteoglycans induces sprouting of intact purkinje axons in the cerebellum of the adult rat. The Journal of Neuroscience: The Official Journal of the Society for Neuroscience, 25(31), 7150–7158. 10.1523/JNEUROSCI.0683-05.2005. [PubMed: 16079397]

Dalla C, Papachristos EB, Whetstone AS, & Shors TJ (2009). Female rats learn trace memories better than male rats and consequently retain a greater proportion of new neurons in their hippocampi. Proceedings of the National Academy of Sciences of the United States of America, 106(8), 2927–2932. 10.1073/pnas.0809650106. [PubMed: 19188598]

Dalla C, & Shors TJ (2009). Sex differences in learning processes of classical and operant conditioning. Physiology & Behavior, 97(2), 229–238. 10.1016/j.physbeh.2009.02.035. [PubMed: 19272397]

De Luca C, & Papa M (2016). Looking Inside the Matrix: Perineuronal Nets in Plasticity, Maladaptive Plasticity and Neurological Disorders. Neurochemical Research, 41(7), 1507–1515. 10.1007/s11064-016-1876-2. [PubMed: 26935742]

de Winter F, Kwok JCF, Fawcett JW, Vo TT, Carulli D, & Verhaagen J (2016). The Chemorepulsive Protein Semaphorin 3A and Perineuronal Net-Mediated Plasticity. Neural Plasticity, 2016, Article e3679545. 10.1155/2016/3679545.

Dehmelt L, & Halpain S (2004). The MAP2/Tau family of microtubule-associated proteins. Genome Biology, 6(1), 204. 10.1186/gb-2004-6-1-204. [PubMed: 15642108]

Dityatev A, Brückner G, Dityateva G, Grosche J, Kleene R, & Schachner M (2007). Activity-dependent formation and functions of chondroitin sulfate-rich extracellular matrix of perineuronal nets. Developmental Neurobiology, 67(5), 570–588. 10.1002/dneu.20361. [PubMed: 17443809]

Edamatsu M, Miyano R, Fujikawa A, Fujii F, Hori T, Sakaba T, & Oohashi T (2018). Hapln4/Bral2 is a selective regulator for formation and transmission of GABAergic synapses between Purkinje and deep cerebellar nuclei neurons. Journal of Neurochemistry, 147(6), 748–763. 10.1111/jnc.14571. [PubMed: 30125937]

Fawcett JW, Oohashi T, & Pizzorusso T (2019). The roles of perineuronal nets and the perinodal extracellular matrix in neuronal function. Nature Reviews Neuroscience, 20(8), 451–465. 10.1038/s41583-019-0196-3. [PubMed: 31263252]

Ferrer-Ferrer M, & Dityatev A (2018). Shaping Synapses by the Neural Extracellular Matrix. Frontiers in Neuroanatomy, 12. 10.3389/fnana.2018.00040.

Freeman JH, Carter CS, & Stanton ME (1995). Early cerebellar lesions impair eyeblink conditioning in developing rats: Differential effects of unilateral lesions on Postnatal Day 10 or 20. Behavioral Neuroscience, 109(5), 893–902. 10.1037/0735-7044.109.5.893. [PubMed: 8554713]

Freeman JH, & Rabinak CA (2005). Eyeblink conditioning in rats using pontine stimulation as a conditioned stimulus. Integrative Physiological and Behavioral Science, 39(3), 180–191. 10.1007/BF02734438.

Galtrey CM, Kwok JCF, Carulli D, Rhodes KE, & Fawcett JW (2008). Distribution and synthesis of extracellular matrix proteoglycans, hyaluronan, link proteins and tenascin-R in the rat spinal cord. European Journal of Neuroscience, 27 (6), 1373–1390. 10.1111/j.1460-9568.2008.06108.x.

Gerwig M, Hajjar K, Frings M, Dimitrova A, Thilmann AF, Kolb FP, … Timmann D (2006). Extinction of conditioned eyeblink responses in patients with cerebellar disorders. Neuroscience Letters, 406(1), 87–91. 10.1016/j.neulet.2006.07.017. [PubMed: 16905257]

Giamanco KA, Morawski M, & Matthews RT (2010). Perineuronal net formation and structure in aggrecan knockout mice. Neuroscience, 170(4), 1314–1327. 10.1016/j.neuroscience.2010.08.032. [PubMed: 20732394]

Glickstein M, Strata P, & Voogd J (2009). Cerebellum: History. Neuroscience, 162(3), 549–559. 10.1016/j.neuroscience.2009.02.054. [PubMed: 19272426]

Gogolla N, Caroni P, Lüthi A, & Herry C (2009). Perineuronal nets protect fear memories from erasure. Science (New York, N.Y.), 325(5945), 1258–1261. 10.1126/science.1174146.

Goldsberry ME, Elkin ME, & Freeman JH (2014). Sensory system development influences the ontogeny of eyeblink conditioning. Developmental Psychobiology, 56 (6), 1244–1251. 10.1002/dev.21204. [PubMed: 24519393]

Guirado R, Perez-Rando M, Sanchez-Matarredona D, Castrén E, & Nacher J (2014). Chronic fluoxetine treatment alters the structure, connectivity and plasticity of cortical interneurons. The International Journal of Neuropsychopharmacology; Oxford, 17(10), 1635–1646. 10.1017/S1461145714000406. [PubMed: 24786752]

Hayani H, Song I, & Dityatev A (2018). Increased Excitability and Reduced Excitatory Synaptic Input Into Fast-Spiking CA2 Interneurons After Enzymatic Attenuation of Extracellular Matrix. Frontiers in Cellular Neuroscience, 12. 10.3389/fncel.2018.00149.

Heiney SA, Wohl MP, Chettih SN, Ruffolo LI, & Medina JF (2014). Cerebellar-Dependent Expression of Motor Learning during Eyeblink Conditioning in Head-Fixed Mice. Journal of Neuroscience, 34(45), 14845–14853. 10.1523/JNEUROSCI.2820-14.2014. [PubMed: 25378152]

Hensch TK (2005). Critical period plasticity in local cortical circuits. Nature Reviews Neuroscience, 6(11), 877–888. 10.1038/nrn1787. [PubMed: 16261181]

Hettiaratchi MH, O'Meara MJ, Teal CJ, Payne SL, Pickering AJ, & Shoichet MS (2019). Local delivery of stabilized chondroitinase ABC degrades chondroitin sulfate proteoglycans in stroke-injured rat brains. Journal of Controlled Release, 297, 14–25. 10.1016/j.jconrel.2019.01.033. [PubMed: 30690102]

Hilbig H, Bidmon HJ, Blohm U, & Zilles K (2001). Wisteria floribunda agglutinin labeling patterns in the human cortex: A tool for revealing areal borders and subdivisions in parallel with immunocytochemistry. Anatomy and Embryology, 203 (1), 45–52. [PubMed: 11195088]

Hirono M, Watanabe S, Karube F, Fujiyama F, Kawahara S, Nagao S, … Misonou H (2018). Perineuronal nets in the deep cerebellar nuclei regulate GABAergic transmission and delay eyeblink conditioning. Journal of Neuroscience, 3238–17. 10.1523/JNEUROSCI.3238-17.2018.

Hou X, Yoshioka N, Tsukano H, Sakai A, Miyata S, Watanabe Y, … Sugiyama S (2017). Chondroitin Sulfate Is Required for Onset and Offset of Critical Period Plasticity in Visual Cortex. Scientific Reports, 7(1), 12646. 10.1038/s41598-017-04007-x. [PubMed: 28974755]

Huang S, & Uusisaari MY (2013). Physiological temperature during brain slicing enhances the quality of acute slice preparations. Frontiers in Cellular Neuroscience, 7, 48. 10.3389/fncel.2013.00048. [PubMed: 23630465]

Iwata M, Wight TN, & Carlson SS (1993). A brain extracellular matrix proteoglycan forms aggregates with hyaluronan. Journal of Biological Chemistry, 268(20), 15061–15069.

Kecskes S, Gaal B, Racz E, Birinyi A, Hunyadi A, & Matesz C (2015). Extracellular Matrix Molecules Exhibit Unique Expression Pattern in the Climbing Fiber-Generating Precerebellar Nucleus, the Inferior Olive. Neuroscience, 284, 412–421. 10.1016/j.neuroscience.2014.09.080. [PubMed: 25445196]

Kindler S, & Garner CC (1994). Four repeat MAP2 isoforms in human and rat brain. Brain Research. Molecular Brain Research, 26(1–2), 218–224. 10.1016/0169-328x(94)90093-0. [PubMed: 7854050]

Koekkoek SKE, Den Ouden WL, Perry G, Highstein SM, & De Zeeuw CI (2002). Monitoring Kinetic and Frequency-Domain Properties of Eyelid Responses in Mice With Magnetic Distance Measurement Technique. Journal of Neurophysiology, 88(4), 2124–2133. 10.1152/jn.2002.88.4.2124. [PubMed: 12364534]

Kreider JC, & Mauk MD (2010). Eyelid Conditioning to a Target Amplitude: Adding How Much to Whether and When. Journal of Neuroscience, 30(42), 14145–14152. 10.1523/JNEUROSCI.3473-10.2010. [PubMed: 20962235]

Krishnaswamy VR, Benbenishty A, Blinder P, & Sagi I (2019). Demystifying the extracellular matrix and its proteolytic remodeling in the brain: Structural and functional insights. Cellular and Molecular Life Sciences. 10.1007/s00018-019-03182-6.

Leuner B, Mendolia-Loffredo S, & Shors TJ (2004). High levels of estrogen enhance associative memory formation in ovariectomized females. Psychoneuroendocrinology, 29(7), 883–890. 10.1016/j.psyneuen.2003.08.001. [PubMed: 15177703]

Massey JM, Hubscher CH, Wagoner MR, Decker JA, Amps J, Silver J, & Onifer SM (2006). Chondroitinase ABC Digestion of the Perineuronal Net Promotes Functional Collateral Sprouting in the Cuneate Nucleus after Cervical Spinal Cord Injury. Journal of Neuroscience, 26(16), 4406–4414. 10.1523/JNEUROSCI.5467-05.2006. [PubMed: 16624960]

Matthews RT, Kelly GM, Zerillo CA, Gray G, Tiemeyer M, & Hockfield S (2002). Aggrecan Glycoforms Contribute to the Molecular Heterogeneity of Perineuronal Nets. Journal of Neuroscience, 22(17), 7536–7547. [PubMed: 12196577]

Matus A, Delhaye-Bouchaud N, & Mariani J (1990). Microtubule-associated protein 2 (MAP2) in Purkinje cell dendrites: Evidence that factors other than binding to microtubules are involved in determining its cytoplasmic distribution. The Journal of Comparative Neurology, 297(3), 435–440. 10.1002/cne.902970308. [PubMed: 2398141]

McDonald AJ, Hamilton PG, & Barnstable CJ (2017). Perineuronal nets labeled by monoclonal antibody VC1.1 ensheath interneurons expressing parvalbumin and calbindin in the rat amygdala. Brain Structure and Function, 1–16. 10.1007/s00429-017-1542-8.

McEchron MD, Tseng W, & Disterhoft JF (2003). Single Neurons in CA1 Hippocampus Encode Trace Interval Duration during Trace Heart Rate (Fear) Conditioning in Rabbit. Journal of Neuroscience, 23(4), 1535–1547. 10.1523/JNEUROSCI.23-04-01535.2003. [PubMed: 12598642]

Miller MJ, Chen N, Li L, Tom B, Weiss C, Disterhoft JF, & Wyrwicz AM (2003). FMRI of the Conscious Rabbit during Unilateral Classical Eyeblink Conditioning Reveals Bilateral Cerebellar Activation. Journal of Neuroscience, 23(37), 11753–11758. 10.1523/JNEUROSCI.23-37-11753.2003. [PubMed: 14684877]

Minta K, Portelius E, Janelidze S, Hansson O, Zetterberg H, Blennow K, & Andreasson U (2019). Cerebrospinal Fluid Concentrations of Extracellular Matrix Proteins in Alzheimer's Disease. Journal of Alzheimer's Disease: JAD. 10.3233/JAD-190187.

Morikawa S, Ikegaya Y, Narita M, & Tamura H (2017). Activation of perineuronal net-expressing excitatory neurons during associative memory encoding and retrieval. Scientific Reports, 7, srep46024. 10.1038/srep46024.

Morris NP, & Henderson Z (2000). Perineuronal nets ensheath fast spiking, parvalbumin-immunoreactive neurons in the medial septum/diagonal band complex. European Journal of Neuroscience, 12(3), 828–838. 10.1046/j.1460-9568.2000.00970.x.

Moyer JR, Power JM, Thompson LT, & Disterhoft JF (2000). Increased excitability of aged rabbit CA1 neurons after trace eyeblink conditioning. The Journal of Neuroscience: The Official Journal of the Society for Neuroscience, 20(14), 5476–5482. [PubMed: 10884331]

Moyer JR, Thompson LT, & Disterhoft JF (1996). Trace eyeblink conditioning increases CA1 excitability in a transient and learning-specific manner. The Journal of Neuroscience: The Official Journal of the Society for Neuroscience, 16(17), 5536–5546. [PubMed: 8757265]

Mueller AL, Davis A, Sovich S, Carlson SS, & Robinson FR (2016). Distribution of N-Acetylgalactosamine-Positive Perineuronal Nets in the Macaque Brain: Anatomy and Implications. Neural Plasticity, 2016, 6021428. 10.1155/2016/6021428. [PubMed: 26881119]

Nabel EM, & Morishita H (2013). Regulating Critical Period Plasticity: Insight from the Visual System to Fear Circuitry for Therapeutic Interventions. Frontiers in Psychiatry, 4. 10.3389/fpsyt.2013.00146.

Nolan BC, Nicholson DA, & Freeman JH (2002). Blockade of GABAA Receptors in the Interpositus Nucleus Modulates Expression of Conditioned Excitation but not Conditioned Inhibition of the Eyeblink Response. Integrative Physiological and Behavioral Science : The Official Journal of the Pavlovian Society, 37(4), 293–310. [PubMed: 12645845]

O'Connor AM, Burton TJ, Mansuri H, Hand GR, Leamey CA, & Sawatari A (2019). Environmental Enrichment From Birth Impacts Parvalbumin Expressing Cells and Wisteria Floribunda Agglutinin Labelled Peri-Neuronal Nets Within the Developing Murine Striatum. Frontiers in Neuroanatomy, 13. 10.3389/fnana.2019.00090.

Oh MM, & Disterhoft JF (2015). Increased Excitability of Both Principal Neurons and Interneurons during Associative Learning: The Neuroscientist.. 10.1177/1073858414537382.

Ohira K, Takeuchi R, Iwanaga T, & Miyakawa T (2013). Chronic fluoxetine treatment reduces parvalbumin expression and perineuronal nets in gamma-aminobutyric acidergic interneurons of the frontal cortex in adult mice. Molecular Brain, 6, 43. 10.1186/1756-6606-6-43. [PubMed: 24228616]

Paxinos G, & Watson C (2004). The Rat Brain in Stereotaxic Coordinates (5th ed.). Elsevier Academic Press, 2005. https://books-google-com.www.libproxy.wvu.edu/books/about/The_Rat_Brain_in_Stereotaxic_Coordinates.html?id=LKJqAAAAMAAJ.

Perciavalle V, Apps R, Bracha V, Delgado-García JM, Gibson AR, Leggio M, … Sánchez-Campusano R (2013). Consensus Paper: Current Views on the Role of Cerebellar Interpositus Nucleus in Movement Control and Emotion. The Cerebellum, 12(5), 738–757. 10.1007/s12311-013-0464-0. [PubMed: 23564049]

Perea G, Navarrete M, & Araque A (2009). Tripartite synapses: Astrocytes process and control synaptic information. Trends in Neurosciences, 32(8), 421–431. 10.1016/j.tins.2009.05.001. [PubMed: 19615761]

Person AL, & Raman IM (2012). Synchrony and neural coding in cerebellar circuits. Frontiers in Neural Circuits, 6, 97. 10.3389/fncir.2012.00097. [PubMed: 23248585]

Pizzorusso T, Medini P, Berardi N, Chierzi S, Fawcett JW, & Maffei L (2002). Reactivation of Ocular Dominance Plasticity in the Adult Visual Cortex. Science, 298 (5596), 1248–1251. 10.1126/science.1072699. [PubMed: 12424383]

Pugh JR, & Raman IM (2006). Potentiation of mossy fiber EPSCs in the cerebellar nuclei by NMDA receptor activation followed by postinhibitory rebound current. Neuron, 51(1), 113–123. 10.1016/j.neuron.2006.05.021. [PubMed: 16815336]

Rakic P (1971). Neuron-glia relationship during granule cell migration in developing cerebellar cortex. A Golgi and electonmicroscopic study in Macacus rhesus. Journal of Comparative Neurology, 141(3), 283–312. 10.1002/cne.901410303.

Rowlands D, Lensjø KK, Dinh T, Yang S, Andrews MR, Hafting T, … Dick G (2018). Aggrecan directs extracellular matrix mediated neuronal plasticity. Journal of Neuroscience, 1122–18. 10.1523/JNEUROSCI.1122-18.2018.

Schreurs BG (2019). Changes in cerebellar intrinsic neuronal excitability and synaptic plasticity result from eyeblink conditioning. Neurobiology of Learning and Memory, 166, Article 107094. 10.1016/j.nlm.2019.107094. [PubMed: 31542329]

Schreurs BG, Burhans LB, Smith-Bell CA, Mrowka SW, & Wang D (2013). Ontogeny of trace eyeblink conditioning to shock-shock pairings in the rat pup. Behavioral Neuroscience, 127(1), 114–120. 10.1037/a0031298. [PubMed: 23244289]

Seeger G, Brauer K, Härtig W, & Brückner G (1994). Mapping of perineuronal nets in the rat brain stained by colloidal iron hydroxide histochemistry and lectin cytochemistry. Neuroscience, 58(2), 371–388. 10.1016/0306-4522(94)90044-2. [PubMed: 7512240]

Shors TJ, & Miesegaes G (2002). Testosterone in utero and at birth dictates how stressful experience will affect learning in adulthood. Proceedings of the National Academy of Sciences of the United States of America, 99(21), 13955–13960. 10.1073/pnas.202199999. [PubMed: 12359876]

Slaker ML, Jorgensen ET, Hegarty DM, Liu X, Kong Y, Zhang F, … Sorg BA (2018). Cocaine Exposure Modulates Perineuronal Nets and Synaptic Excitability of Fast-Spiking Interneurons in the Medial Prefrontal Cortex. ENeuro, 5(5). 10.1523/ENEURO.0221-18.2018.

Smith-Bell CA, Burhans LB, & Schreurs BG (2012). Predictors of susceptibility and resilience in an animal model of posttraumatic stress disorder. Behavioral Neuroscience, 126(6), 749–761. 10.1037/a0030713. [PubMed: 23181382]

Smith-Bell CA, & Schreurs BG (2017). Grouping subjects based on conditioning criteria reveals differences in acquisition rates and in strength of conditioning-specific reflex modification. Neurobiology of Learning and Memory, 145, 172–180. 10.1016/j.nlm.2017.10.004. [PubMed: 29031809]

Sorg BA, Berretta S, Blacktop JM, Fawcett JW, Kitagawa H, Kwok JCF, & Miquel M (2016). Casting a Wide Net: Role of Perineuronal Nets in Neural Plasticity. Journal of Neuroscience, 36(45), 11459–11468. 10.1523/JNEUROSCI.2351-16.2016. [PubMed: 27911749]

Stamenkovic V, Stamenkovic S, Jaworski T, Gawlak M, Jovanovic M, Jakovcevski I, … Andjus PR (2017). The extracellular matrix glycoprotein tenascin-C and matrix metalloproteinases modify cerebellar structural plasticity by exposure to an enriched environment. Brain Structure & Function, 222(1), 393–415. 10.1007/s00429-016-1224-y. [PubMed: 27089885]

Stanton ME, Freeman JH, & Skelton RW (1992). Eyeblink conditioning in the developing rat. Behavioral Neuroscience, 106(4), 657–665. 10.1037/0735-7044.106.4.657. [PubMed: 1503658]

Steinmetz JE, Lavond DG, & Thompson RF (1989). Classical conditioning in rabbits using pontine nucleus stimulation as a conditioned stimulus and inferior olive stimulation as an unconditioned stimulus. Synapse, 3(3), 225–233. 10.1002/syn.890030308. [PubMed: 2718098]

Stryker C, Camperchioli DW, Mayer CA, Alilain WJ, Martin RJ, & MacFarlane PM (2017). Respiratory dysfunction following neonatal sustained hypoxia exposure during a critical window

of brainstem extracellular matrix formation. American Journal of Physiology. Regulatory, Integrative and Comparative Physiology, ajpregu.00199.2017. 10.1152/ajpregu.00199.2017.

Sun ZY, Bozzelli PL, Caccavano A, Allen M, Balmuth J, Vicini S, … Conant K (2018). Disruption of perineuronal nets increases the frequency of sharp wave ripple events. Hippocampus, 28(1), 42–52. 10.1002/hipo.22804. [PubMed: 28921856]

Suttkus A, Holzer M, Morawski M, & Arendt T (2016). The neuronal extracellular matrix restricts distribution and internalization of aggregated Tau-protein. Neuroscience, 313(Supplement C), 225–235. 10.1016/j.neuroscience.2015.11.040. [PubMed: 26621125]

Thompson RF, & Steinmetz JE (2009). The role of the cerebellum in classical conditioning of discrete behavioral responses. Neuroscience, 162(3), 732–755. 10.1016/j.neuroscience.2009.01.041. [PubMed: 19409234]

Tucker R, Binder L, Viereck C, Hemmings B, & Matus A (1988). The sequential appearance of low- and high-molecular-weight forms of MAP2 in the developing cerebellum. The Journal of Neuroscience, 8(12), 4503–4512. 10.1523/JNEUROSCI.08-12-04503.1988. [PubMed: 3199190]

Umemori J, Winkel F, Castrén E, & Karpova NN (2015). Distinct effects of perinatal exposure to fluoxetine or methylmercury on parvalbumin and perineuronal nets, the markers of critical periods in brain development. International Journal of Developmental Neuroscience: The Official Journal of the International Society for Developmental Neuroscience, 44, 55–64. 10.1016/j.ijdevneu.2015.05.006. [PubMed: 25997908]

Waddell J, Mallimo E, & Shors T (2010). D-cycloserine reverses the detrimental effects of stress on learning in females and enhances retention in males. Neurobiology of Learning and Memory, 93(1), 31–36. 10.1016/j.nlm.2009.08.002. [PubMed: 19666130]

Wang D, & Schreurs BG (2010). Dietary cholesterol modulates the excitability of rabbit hippocampal CA1 pyramidal neurons. Neuroscience Letters, 479(3), 327–331. 10.1016/j.neulet.2010.05.090. [PubMed: 20639007]

Wang D, & Schreurs BG (2014). Maturation of membrane properties of neurons in the rat deep cerebellar nuclei. Developmental Neurobiology, 74(12), 1268–1276. 10.1002/dneu.22203. [PubMed: 24931427]

Wang D, Smith-Bell CA, Burhans LB, O'Dell DE, Bell RW, & Schreurs BG (2018). Changes in membrane properties of rat deep cerebellar nuclear projection neurons during acquisition of eyeblink conditioning. Proceedings of the National Academy of Sciences, 115(40), E9419–E9428. 10.1073/pnas.1808539115.

Wang D, & Zheng W (2015). Dietary cholesterol concentration affects synaptic plasticity and dendrite spine morphology of rabbit hippocampal neurons. Brain Research, 1622, 350–360. 10.1016/j.brainres.2015.06.049. [PubMed: 26188241]

Welsh JP (1992). Changes in the motor pattern of learned and unlearned responses following cerebellar lesions: A kinematic analysis of the nictitating membrane reflex. Neuroscience, 47(1), 1–19. 10.1016/0306-4522(92)90116-J. [PubMed: 1579204]

Xue Y-X, Xue L-F, Liu J-F, He J, Deng J-H, Sun S-C, … Lu L (2014). Depletion of Perineuronal Nets in the Amygdala to Enhance the Erasure of Drug Memories. Journal of Neuroscience, 34(19), 6647–6658. 10.1523/JNEUROSCI.5390-13.2014. [PubMed: 24806690]

Zheng N, & Raman IM (2010). Synaptic inhibition, excitation, and plasticity in neurons of the cerebellar nuclei. Cerebellum (London, England), 9(1), 56–66. 10.1007/s12311-009-0140-6.

Zheng N, & Raman IM (2011). Prolonged Postinhibitory Rebound Firing in the Cerebellar Nuclei Mediated by Group I Metabotropic Glutamate Receptor Potentiation of L-Type Calcium Currents. Journal of Neuroscience, 31(28), 10283–10292. 10.1523/JNEUROSCI.1834-11.2011. [PubMed: 21753005]

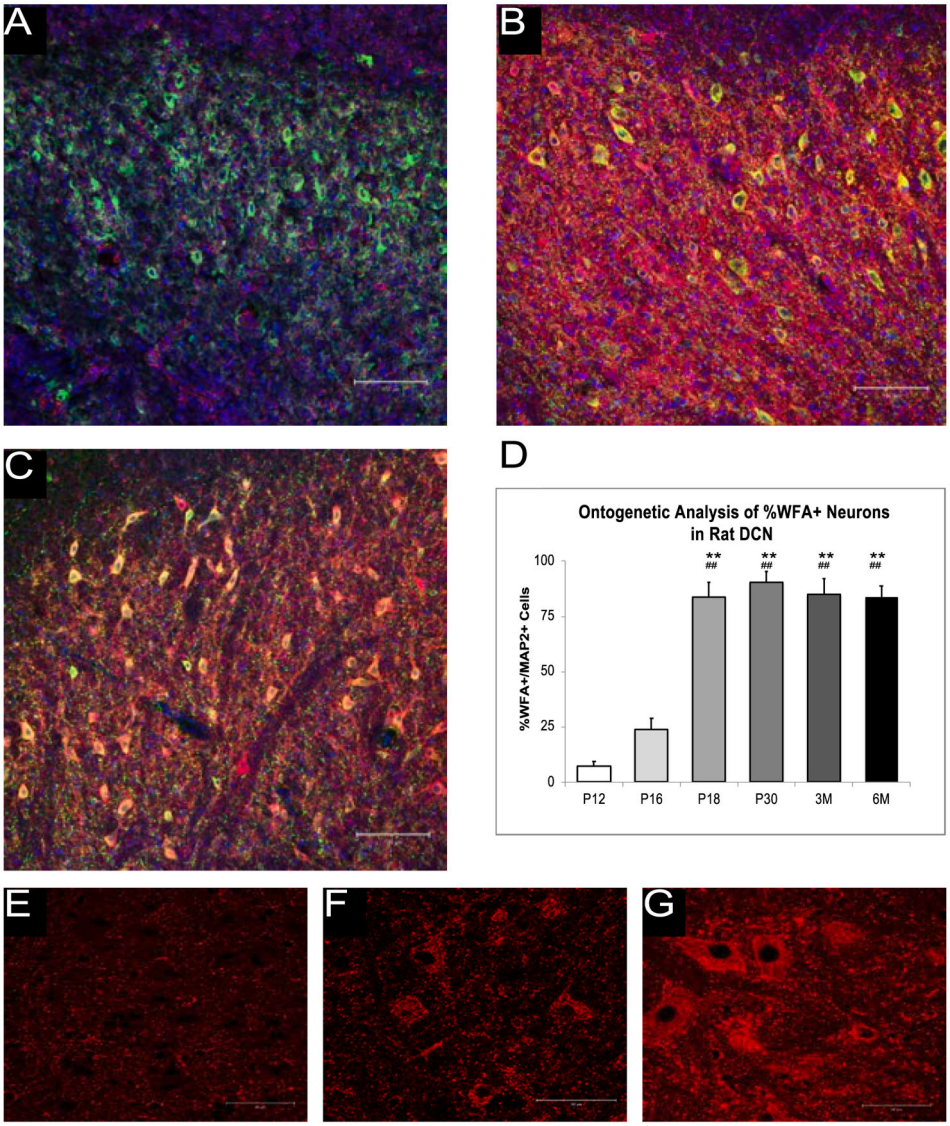

Fig. 1.

Ontogeny of the PNN in the AIN. A-C. shows the WFA reactivity (red), DAPI (blue), and MAP2 reactivity (green) in the rat AIN at P12 (A), P18 (B), and P30 (C) at 20x. D. shows the WFA reactivity at the studied ontogenetic timepoints. There is an increase in the WFA reactivity between P12 and P18 but no significant changes found after this point. E-G show WFA reactivity alone at P12 (E), P30 (F), 3 months (G) at 63x. ** = $p < .01$ at P12, ## = $p < .01$ at P16.

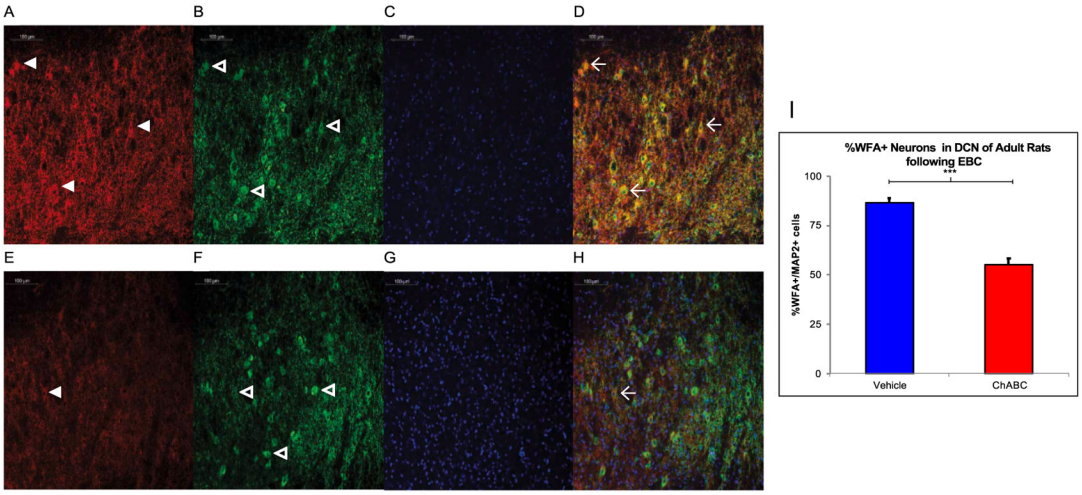

Fig. 2.

In Vivo Digestion of the PNN following EBC. A-D. Rats infused with vehicle show high WFA (red, panel A) reactivity with some PNN noted with white arrowheads as well as MAP2 reactive neurons (green, panel B) with some neurons noted with the open arrowheads and DAPI (blue, panel C) with all four channels merged in D. Three WFA+ neurons are marked with the winged arrowhead in D. E-H. Rats infused with ChABC have less WFA (red, panel E) labeling in comparison and in the merged image, there is only one WFA+ cell. I. A two-tailed unpaired *t*-test found ChABC infusion prior to EBC successfully decreased WFA reactivity in the adult rat AIN. *** = $p < 0.001$.

Fig. 3. Behavioral Timeline.

A simple schematic showing the timeline of the behavioral experiments. Animals had 1 session of tone-shock acquisition for 5 days. 24 h later they had 1 session of extinction for 3 days. 2 weeks post-surgery the animals were given transcardial perfusion for tissue processing.

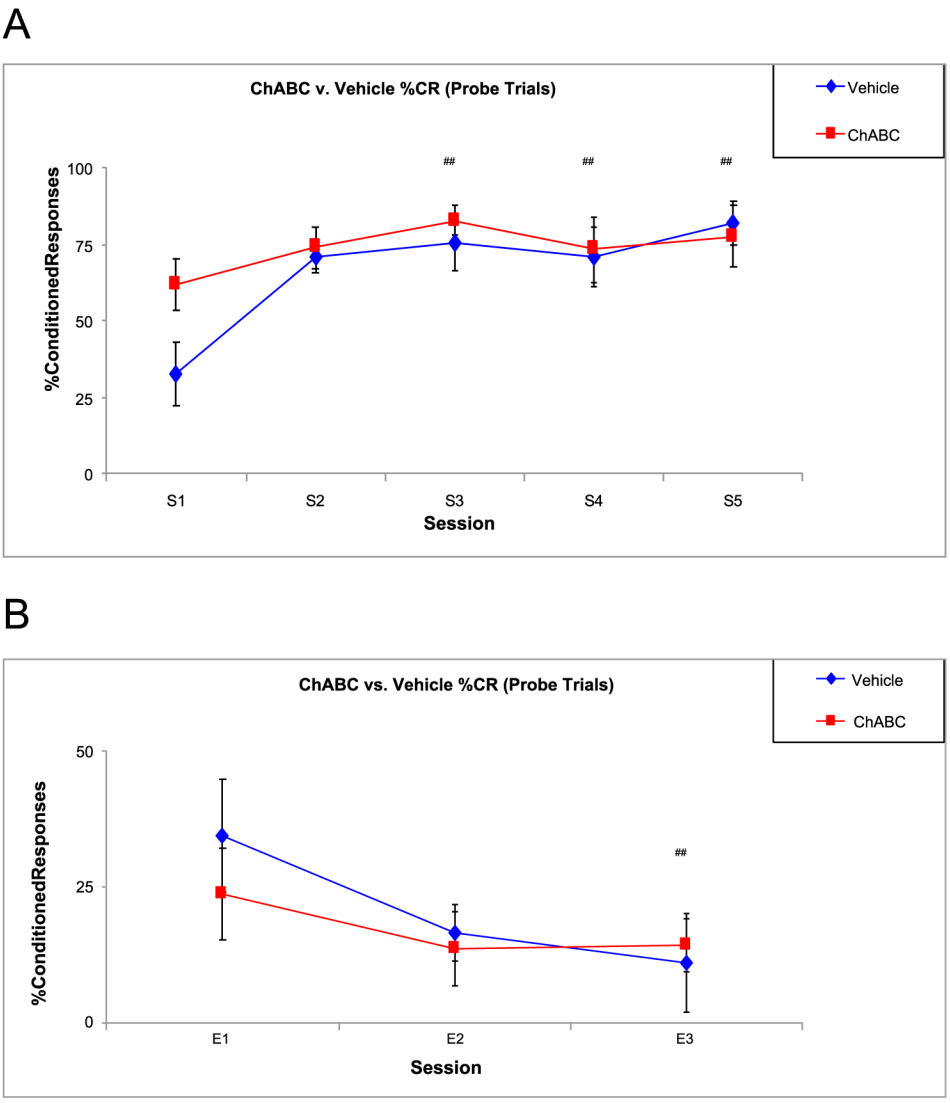

Fig. 4.

Percent Conditioned Responses between ChABC and Vehicle Rats during Acquisition. A. There were no significant differences in %CRs between the two groups but there were significant sessions differences, showing both groups are capable of learning EBC. B. There were differences between sessions during extinction. ## = $p < .05$ for session.

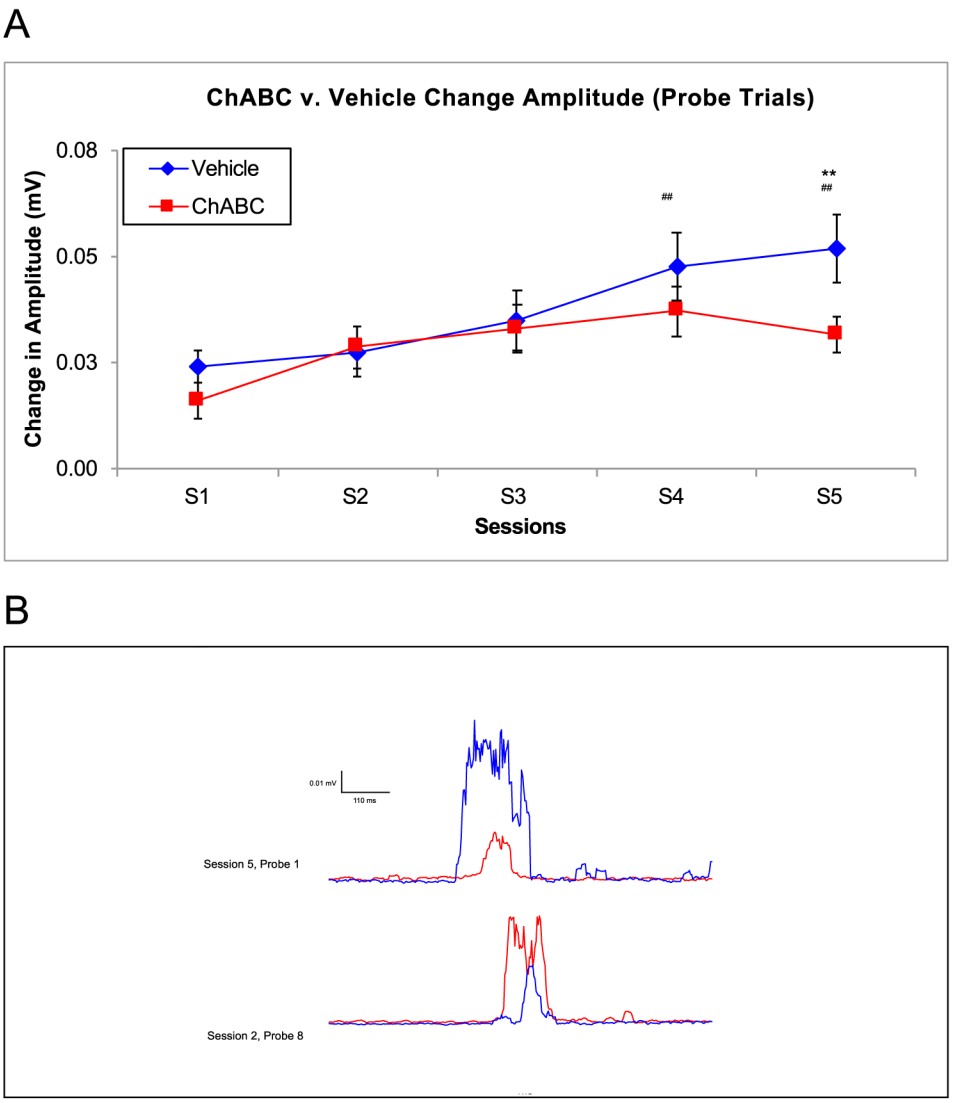

Fig. 5.

Amplitude of the Conditioned Response between ChABC and Vehicle Rats. A. On S5, the vehicle group had a noticeably higher amplitude on the final acquisition session. There were also significant session differences on S4 and S5 showing the amplitude size significantly increased over the acquisition period. B. the amplitude of a vehicle and ChABC infused rat changed from S3 (bottom traces) to S5 (top trace). ## = $p < .05$ for session, ** = $p < .01$.

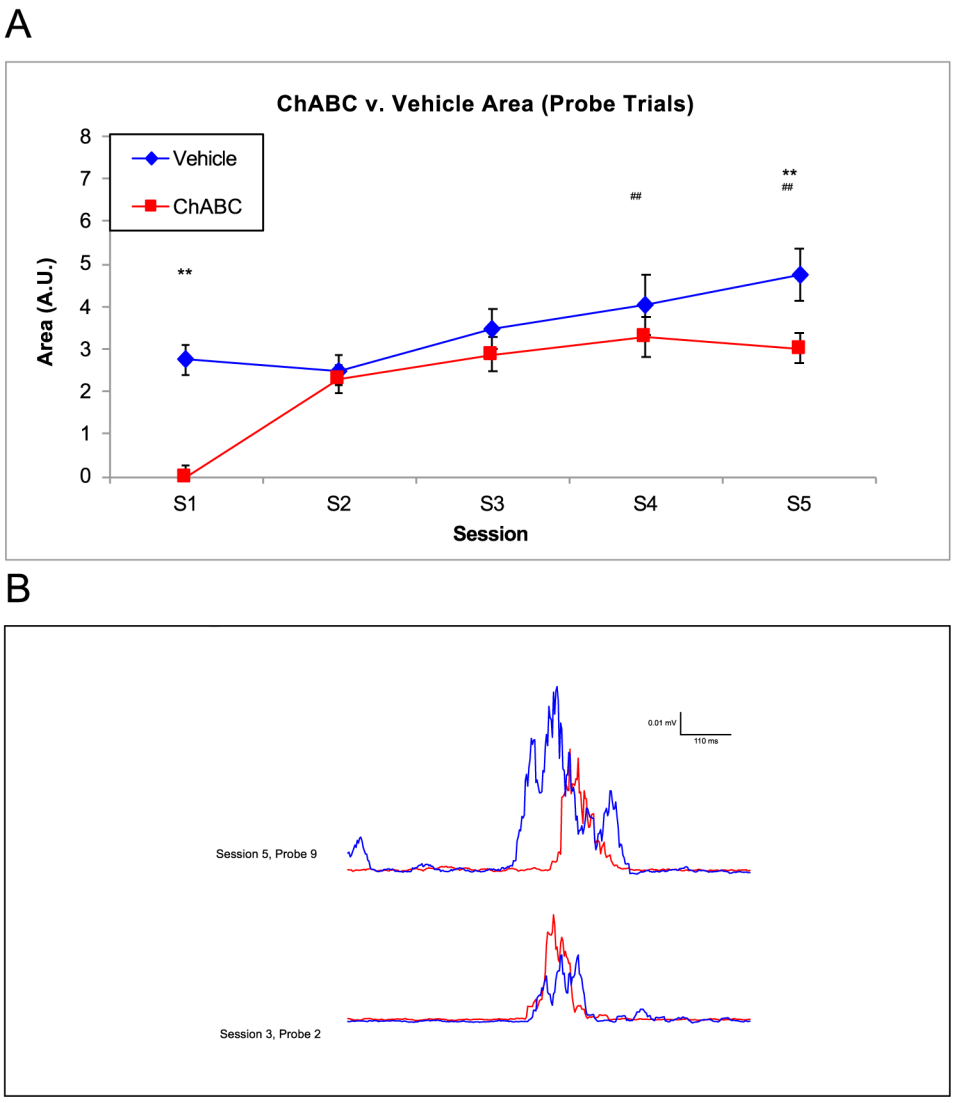

Fig. 6.

Area of the Conditioned Response between ChABC and Vehicle Rats. A. On both S1 and S5, the vehicle group had a noticeably higher area under the curve. B. The area of a vehicle and ChABC infused rat changed from S3 (bottom traces) to S5 (top trace). ## = $p < .05$ for session, ** = $p < .01$.

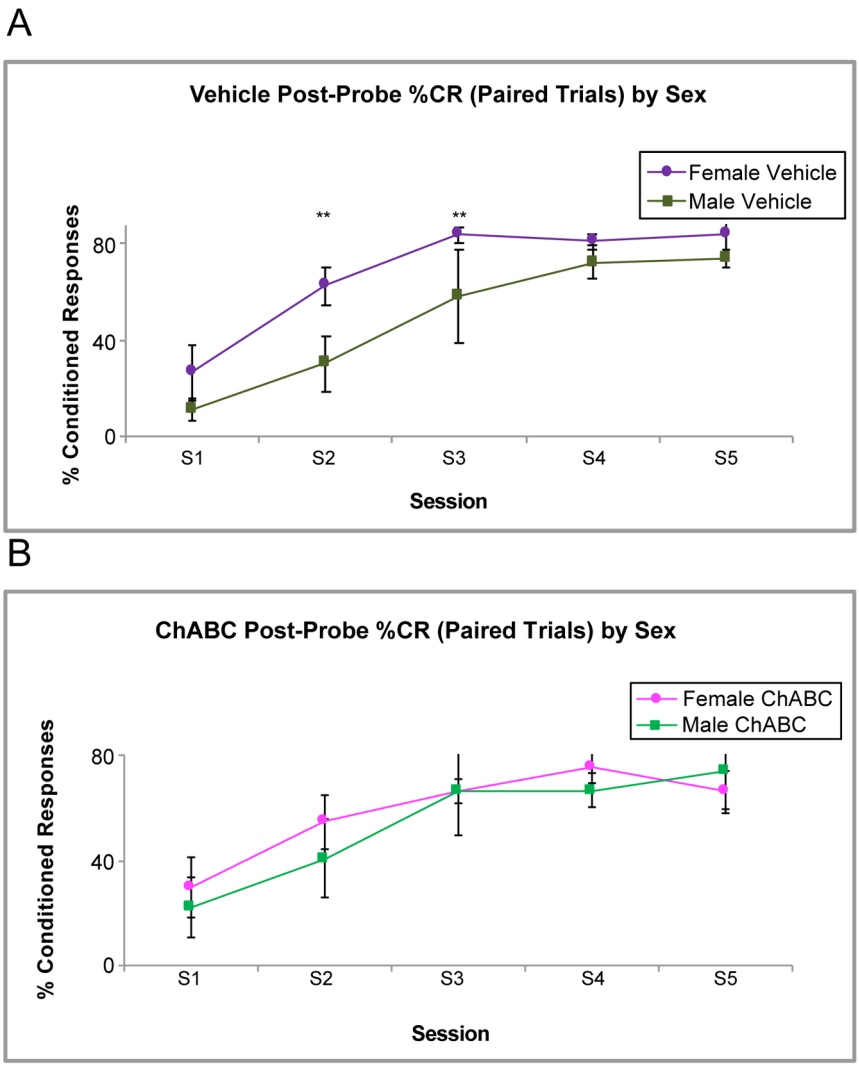

Fig. 7.

%CR Sex Differences between ChABC and Vehicle Rats during Acquisition. A. shows female rats in the vehicle group have higher %CRs compared to their male counterparts on the first tone-shock trials that follow a probe trial. B. shows that this difference is not present in the rats infused with ChABC. ** - $p < .01$.

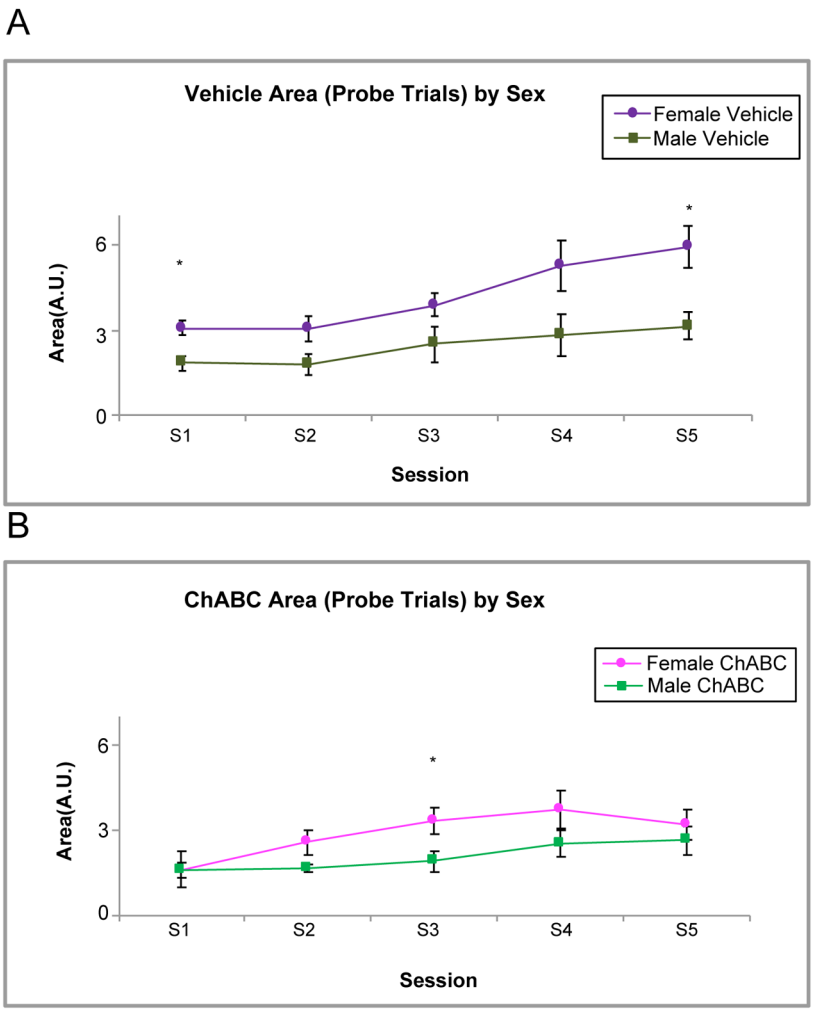

Fig. 8.

Area Sex Differences between ChABC and Vehicle Rats during Acquisition. A. shows female rats in the vehicle group have higher area compared to their male counterparts on probe trials on S1 and S5. B. shows that female rats infused with ChABC also have a higher area than their male counterparts on S3. * - $p < .05$.

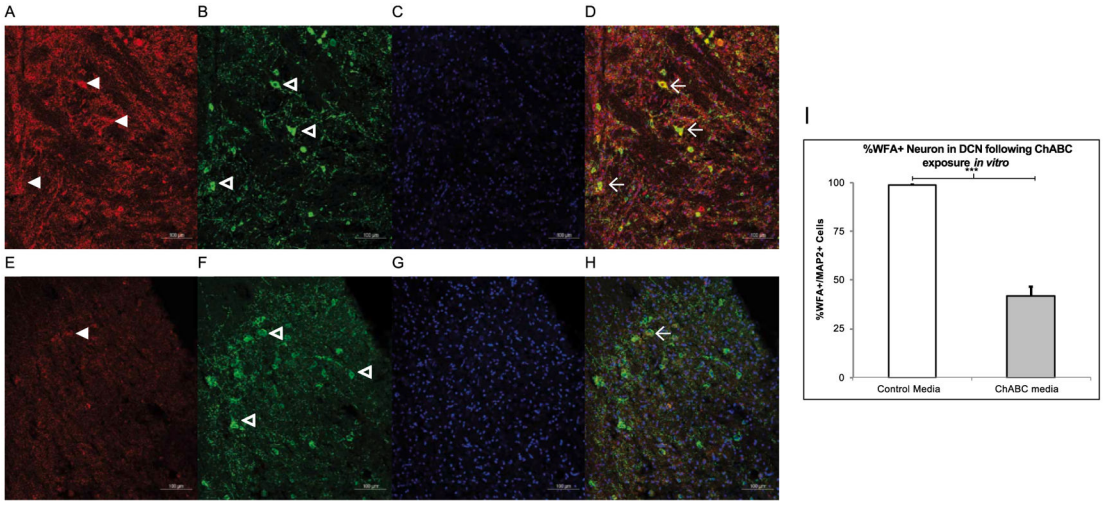

Fig. 9.

In Vitro Digestion of the PNN. A-D. Slices exposed with vehicle show high WFA (red, panel A) reactivity as well as MAP2 reactive neurons (green, panel B) and DAPI (blue, panel C) and all channels merged in D. Three WFA+ neurons are marked with the winged arrowhead in D. E-H. Slices exposed with ChABC have less WFA (red, panel E) labeling in comparison and in the merged image, there is only one WFA+ cell. I. A two-tailed paired *t*-test found ChABC exposure in the electrophysiological bath successfully decreased WFA reactivity in the juvenile rat AIN. *** = $p < 0.001$.

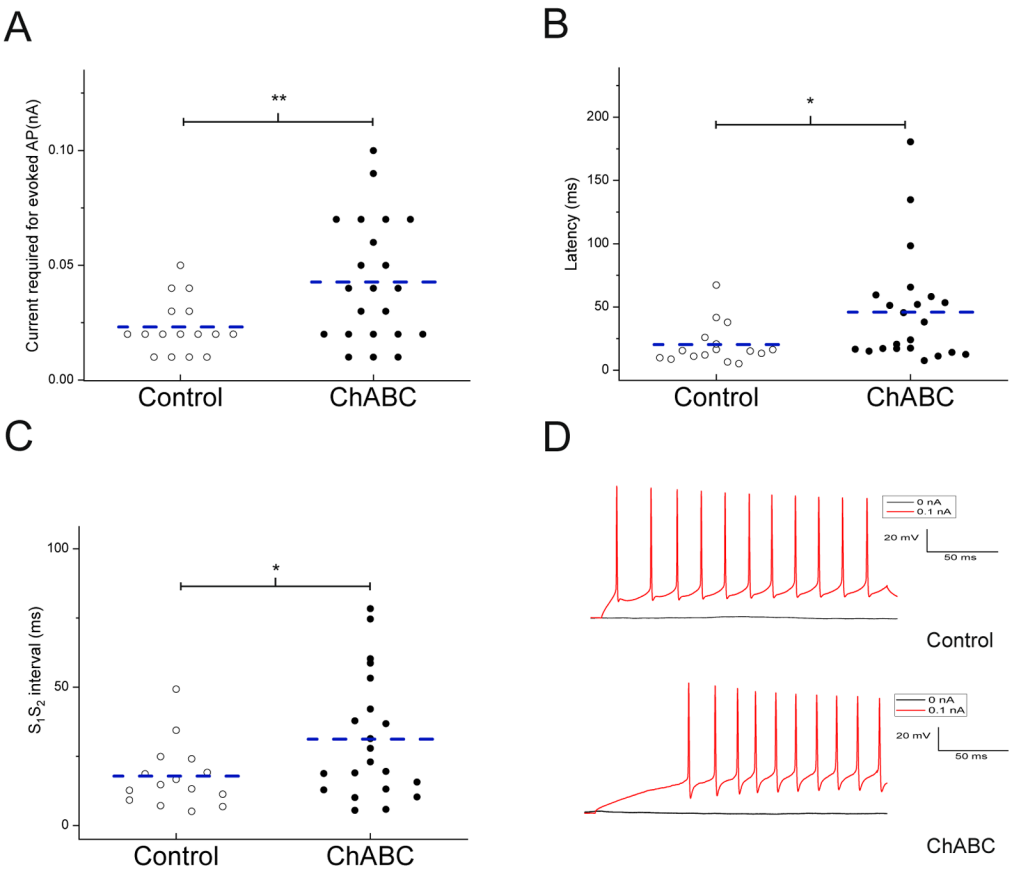

Fig. 10.

ChABC altered the electrophysiological properties of AIN cells. A. shows a higher current is required to evoke an action potential in neurons from ChABC exposed slices. B. shows a significantly longer latency for evoked action potential in neurons from ChABC exposed slices. C. shows a longer S1S2 interval for evoked action potentials in neurons from ChABC exposed slices. D. The typical recordings of action potentials from neurons either in ChABC exposed slices or control medium exposed slices, which were elicited in response to a depolarizing current of 0.1nA. The dashed line indicates the mean. * = $p < .05$, ** = $p < .01$.

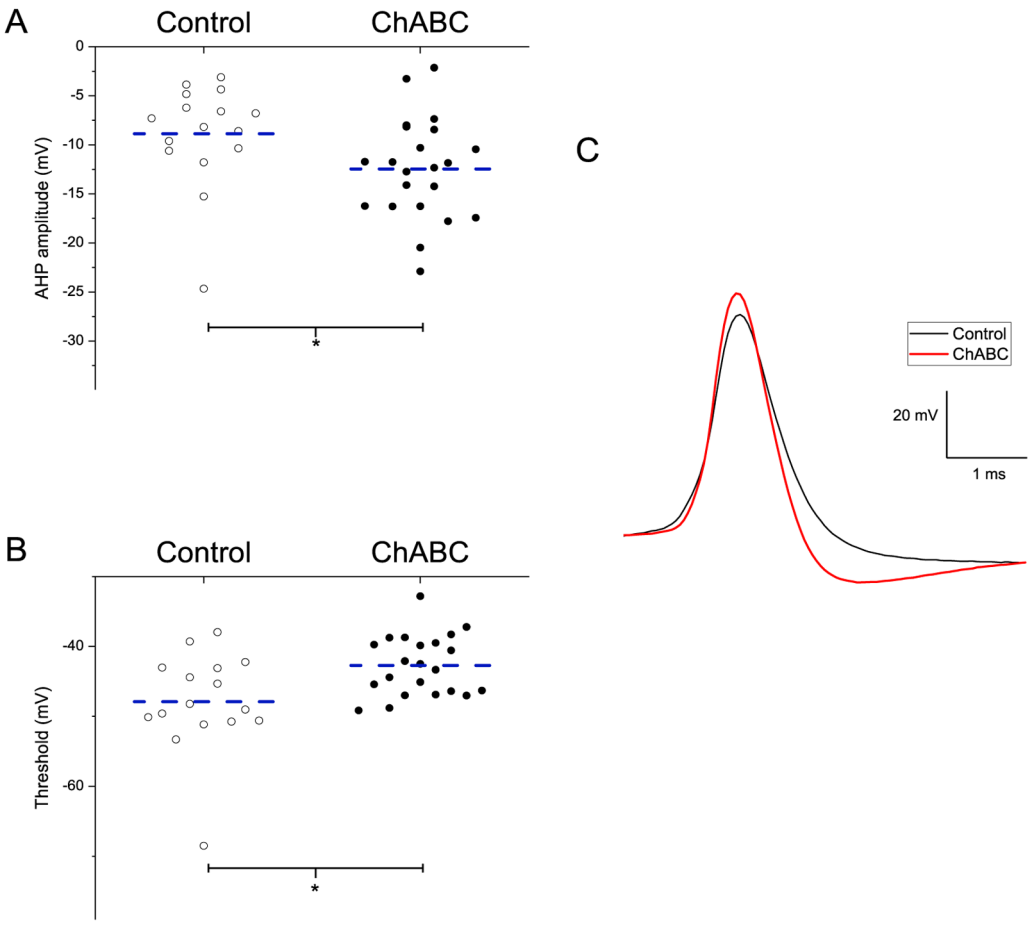

Fig. 11.

ChABC exposure altered the electrophysiological properties of AIN cells. A. shows a larger AHP amplitude for evoked action potential in neurons from ChABC exposed slices. B. shows a lower threshold for evoked action potential in neurons from ChABC exposed slices. C. The traces show ChABC exposed neurons had a larger AHP amplitude compared to control. The dashed line indicated the mean. * = $p < .05$,

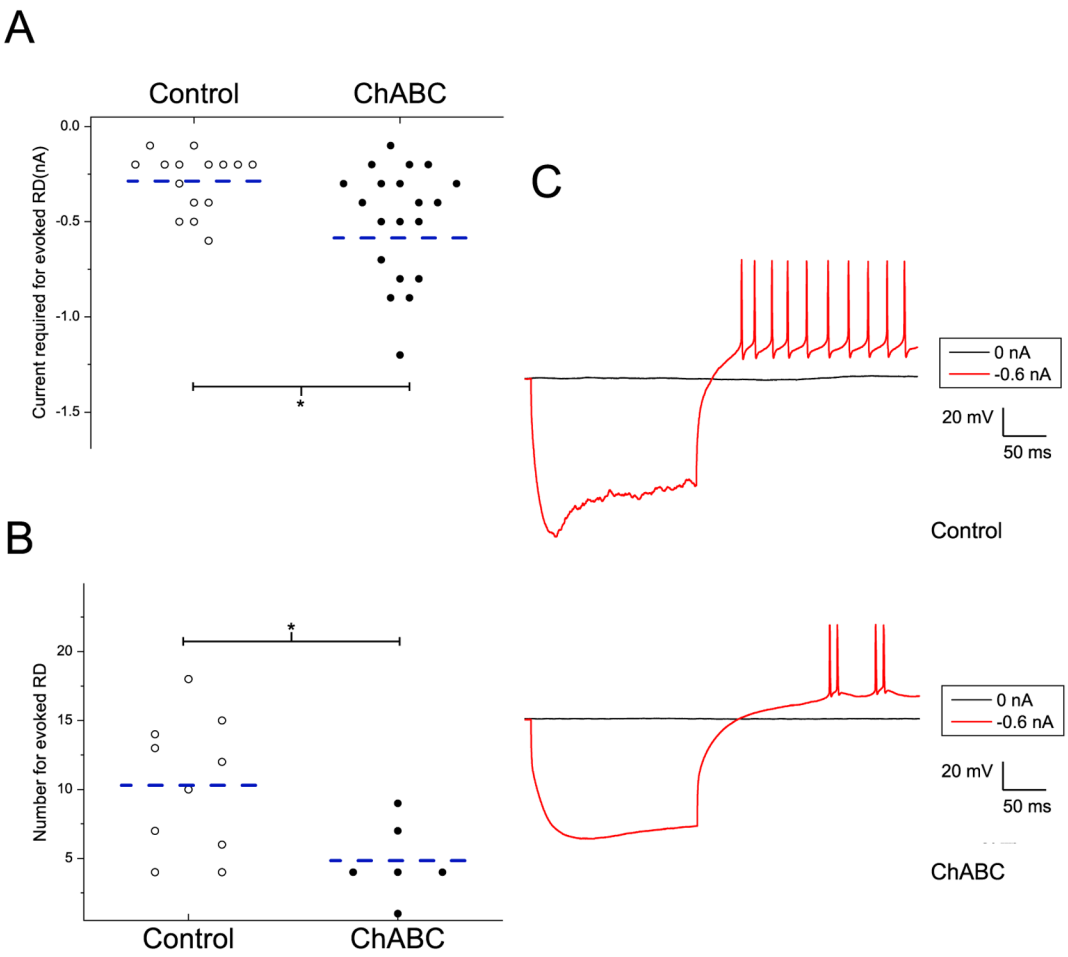

Fig. 12.

ChABC exposure changed the properties of hyperpolarization induced rebound spikes in AIN cells. A. shows a higher current is required to evoke a rebound spike in neurons from ChABC exposed slices. B. shows a lower number of evoked rebound spikes in neurons from ChABC exposed slices. Dashed lines indicate the mean. C. The typical recording of rebound spikes from neurons either in ChABC exposed slices or control medium exposed slices, which were elicited in response to a hyperpolarizing current of −0.6 nA. * = $p < .05$.

Table 1

Materials used in Tissue Processing.

Item (manufacturer)
Chondroitinase ABC (Sigma, cat#: C3667)
Biotin conjugated wisteria floribunda lectin (EY Laboratories Inc., cat#: BA-3101-1) (1:1000)
PSD-95 (Thermofisher Scientific, cat#: MA1-046) (1:2000)
Gephyrin B-4 (Santa Cruz Biotech, cat#: sc-55469) (1:400)
Anti-MAP2, clone AP20 (EMD Millipore, cat#: MAB3418) (1:200)
Donkey Anti-goat A488 (Thermofisher Scientific Inc., Invitrogen, cat#: A-11055) (1:500)
Goat Anti-mouse A546 (Thermofisher Scientific Inc., Invitrogen, cat#: A-21045) (1:500)
Goat Anti-mouse A488 (Thermofisher Scientific Inc., Invitrogen, cat#: A-11029) (1:500)
Streptavidin, Alexa Fluor 647 conjugate (Thermofisher Scientific Inc., Invitrogen, cat#: S-21374) (1:500)
Normal donkey serum (Millpore Sigma, cat#: S30-100KC)
Normal goat serum (Thermofisher Scientific Inc., Gibco, cat#: PCN5000)
Bovine serum albumin (Millipore Sigma, cat#: A3294)
DAPI Fluoromount G (SouthernBiotech, cat#: 0100-20)

Table 2

ChABC treatment altered membrane properties of rat DCN neurons.

	Vm (mV)	Input Res (MΩ)	AP threshold (mV)	Current required for evoked AP (nA)	Latency (ms)	Amplitude (mV)	APD_{50} (ms)	APD_{50} rising (ms)	APD_{50} falling (ms)	AHP (mV)	S1S2 interval (ms)
Vehide	−46.93 ± 0.82	132.95 ± 15.6	**−47.90 ± 1.84**	**0.02 ± 0.01**	**20.27 ± 4.19**	69.92 ± 3.38	1.04 ± 0.16	0.40 ± 0.05	0.64 ± 0.12	**−8.88 ± 1.36**	**17.83 ± 3.14**
ChABC	−46.40 ± 0.69	124.03 ± 1.07	**−42.71 ± 0.94** **	**0.04 ± 0.01** **	**45.99 ± 9.51** *	70.62 ± 2.19	0.97 ± 0.05	0.38 ± 0.02	0.59 ± 0.03	**−12.46 ± 1.12** *	**31.2 ± 5.00** *

Vehicle: Medium treatment; ChABC: ChABC treatment.

Cell number (n) for Vehicle and ChABC was 16, and 22, respectively. Cells from 5 rats.

Note that there were group differences in threshold, current required for evoked AP, latency for evoked AP, AHP amplitude, and S1S2 interval.

*, ** indicate $p < 0.05$, 0.01, respectively.

AP: Action potential; AP duration was measured at the width of 50% AP duration (APD_{50}); AHP: Afterhyperpolarization; Input Res: Input resistance.

Table 3

ChABC treatment affected the properties of rebound spikes from rat DCN neurons.

	Current required for evoked RD (nA)	RD threshold (mV)	RD Amplitude (mV)	RD duration (ms)	RD rising duration (ms)	RD falling duration (ms)	AHP (mV)	S1S2 interval (ms)
Vehide	**−0.29 ± 0.04**	−50.89 ± 1.90	66.49 ± 2.22	0.94 ± 0.11	0.38 ± 0.04	0.56 ± 0.07	−12.22 ± 1.22	33.48 ± 9.60
ChABC	**−0.59 ± 0.11** *	−49.03 ± 1.58	69.39 ± 3.31	1.02 ± 0.06	0.39 ± 0.02	0.60 ± 0.04	−10.73 ± 1.41	44.28 ± 10.59

Vehicle: Medium treatment; ChABC: ChABC treatment.

Cell number (n) for Vehicle and ChABC was 15, and 20, respectively. Cells from 5 rats.

Note that there was difference in Current required for evoked rebound spikes ($p = 0.0339$).

* indicates $p < 0.05$.

RD: Rebound spike; RD duration was measured at the width of 50% RD duration; AHP: Afterhyperpolarization.